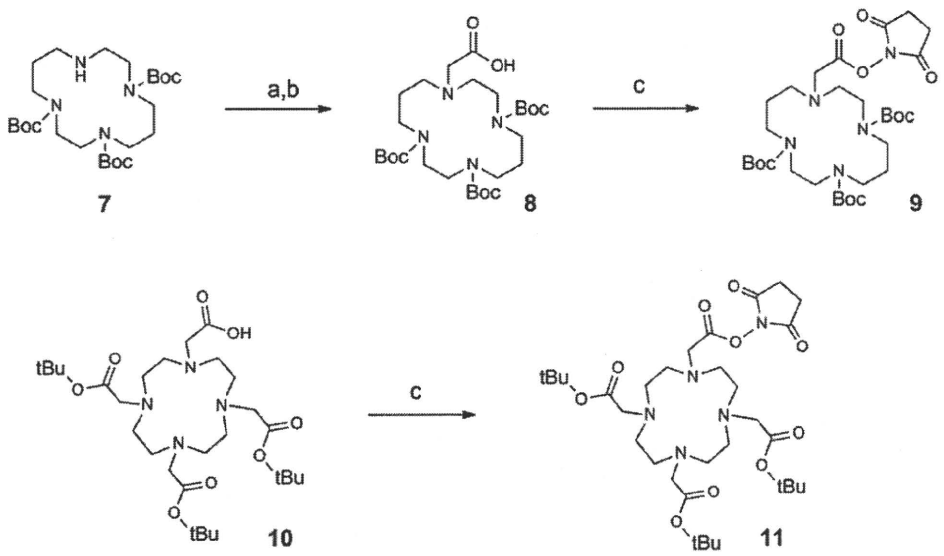

Scheme 2. Reagents and conditions: (a) $BrCH_2CO_2Et$, Na_2CO_3, CH_3CN, 85 °C, 16 h; (b) NaOH, MeOH, 5 h; (c) NHS (1.4 equiv), DCC (1 equiv), AcOH/dioxane (1:1), 5 h.

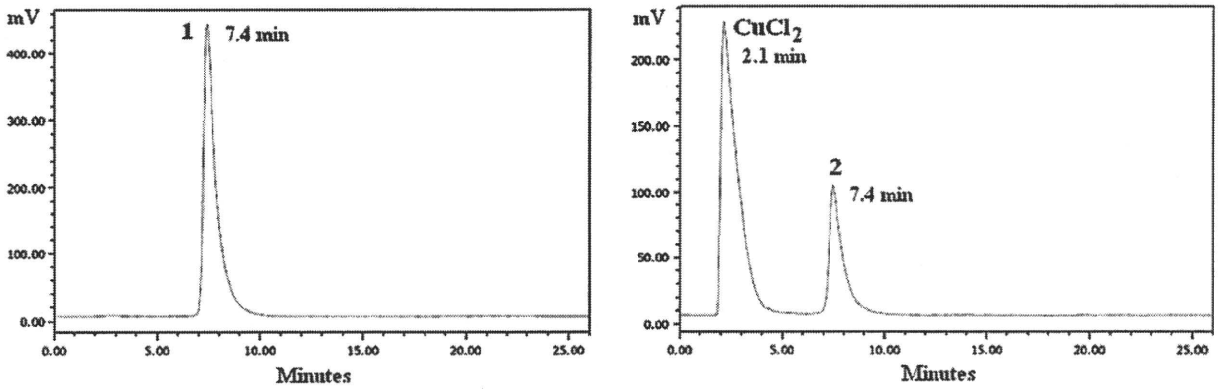

Figure 2. HPLC traces at 1 h for ^{64}Cu labelling of **1** (left chromatogram) and **2** (right chromatogram).

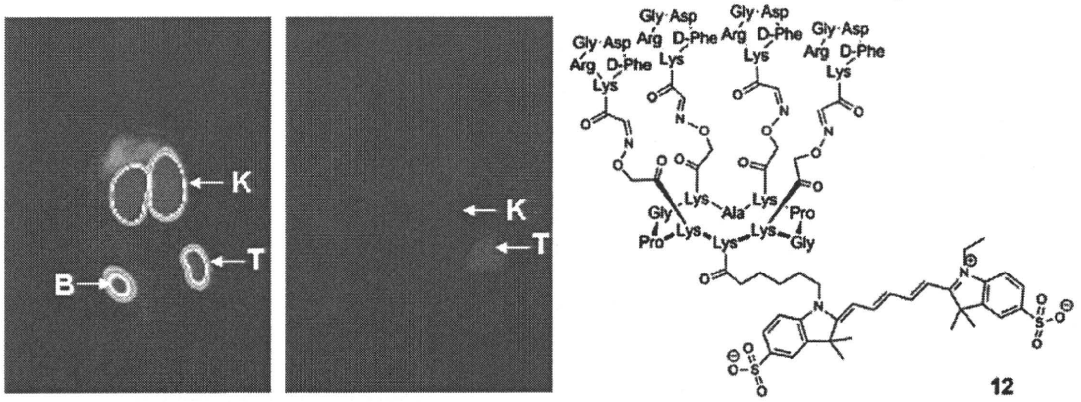

Figure 3. PET and optical image at 5 h of athymic nude mouse bearing subcutaneous $\alpha_v\beta_3$ (+) HEK(β_3) tumour. Mouse received tail vein injection (iv) of 3.7 MBq of ^{64}Cu radiotracer **1** (left) and 3 days later, iv injection of 10 nM of **12** (right). K = kidney, B = bladder, T = tumour.

expected, significant retention of radioactivity was found in kidneys and bladder. This result corroborates previous findings on Cy5-containing fluorescent probes **12** rapidly evacuated with urine.[14,15] Urine samples collected from mice at 4 h post-injection were analyzed and no free copper or Cu–cyclam complex was detected but a major compound that we assume to be a partially degraded peptide and a small amount of radiotracer **1**. Detailed in vivo metabolic stability studies will be evaluated in further study.

After 3 days, the same mouse was injected with RGD-containing fluorescent probe **12** (Fig. 3). The latter was extensively used for the in vivo optical imaging of tumour in mice[8] and successfully exploited for the intraoperative near-infrared image-guided surgery.[16] Optical imaging at 5 h post-injection of **12** shows the accumulation of clustered RGD compound within subcutaneous HEK(β_3) tumour and confirms that the selective targeting of tumour arises from RGD moieties. Further biodistribution studies in mice bearing HEK(β_3) or HEK(β_1) tumours demonstrate that ^{64}Cu radiotracer **1** had much lower radioactivity accumulation in $\alpha_v\beta_3$-negative HEK(β_1) tumours (see Supplementary data). This result reinforces the selectivity of the targeting domain of ^{64}Cu radiotracer **1** for $\alpha_v\beta_3$ integrin.

In conclusion, we used a flexible and modular chemical strategy that gives access to the synthesis of radiotracers in good yields. From basic in vivo studies, ^{64}Cu radiotracer **1** allowed the non-invasive nuclear imaging of $\alpha_v\beta_3$ integrin-expressing tumours. This study emphasizes the use of Copper-64-based radiopharmaceuticals as potential oncological PET imaging agent, and further studies are currently carried out to determine the potential of ^{64}Cu radiotracer **1** for clinical imaging.

Acknowledgements

This work was supported by the Université Joseph Fourier, the Centre National de la Recherche Scientifique (CNRS) and NanoBio (Grenoble).

Supplementary data

Supplementary data associated with this article can be found, in the online version, at doi:10.1016/j.bmcl.2010.07.114.

References and notes

1. Beer, A. J.; Schwaiger, M. *Cancer Metastasis Rev.* **2008**, *27*, 631.
2. Wu, Y.; Zhang, X. Z.; Xiong, Z. M.; Cheng, Z.; Fisher, D. R.; Liu, S.; Gambhir, S. S.; Chen, X. Y. *J. Nucl. Med.* **2005**, *46*, 1707.
3. Liu, S.; Hsieh, W. Y.; Jiang, Y.; Kim, Y. S.; Sreerama, S. G.; Chen, X. Y.; Jia, B.; Wang, F. *Bioconjug. Chem.* **2007**, *18*, 438.
4. Johansson, L. O.; Bjornerud, A.; Ahlstrom, H. K.; Ladd, D. L.; Fujii, D. K. *J. Magn. Reson. Imaging* **2001**, *13*, 615.
5. Chen, X. Y.; Conti, P. S.; Moats, R. A. *Cancer Res.* **2004**, *64*, 8009.
6. Liu, S. *Bioconjug. Chem.* **2009**, *20*, 2199.
7. (a) Maynard, H. D.; Okada, S. Y.; Grubbs, R. H. *J. Am. Chem. Soc.* **2001**, *123*, 1275; (b) Kok, R. J.; Schraa, A. J.; Bos, E. J.; Moorlag, H. E.; Ásgeirsdóttir, S. A.; Everts, M.; Meijer, D. K. F.; Molema, G. *Bioconjug. Chem.* **2002**, *13*, 128; (c) Thumshirn, G.; Hersel, U.; Goodman, S. L.; Kessler, H. *Chem. Eur. J.* **2003**, *9*, 2717; (d) Boturyn, D.; Coll, J.-L.; Garanger, E.; Favrot, M.-C.; Dumy, P. *J. Am. Chem. Soc.* **2004**, *126*, 5730; (e) Montet, X.; Funovics, M.; Montet-Abou, K.; Weissleder, R.; Josephson, L. *J. Med. Chem.* **2006**, *49*, 6087.
8. (a) Jin, Z.; Razkin, J.; Josserand, V.; Boturyn, D.; Grichine, A.; Texier, I.; Favrot, M.-C.; Dumy, P.; Coll, J.-L. *Mol. Imaging* **2007**, *6*, 43; (b) Sancey, L.; Ardisson, V.; Riou, L. M.; Ahmadi, M.; Marti-Batlle, D.; Boturyn, D.; Dumy, P.; Fagret, D.; Ghezzi, C.; Vuillez, J.-P. *Eur. J. Nucl. Med. Mol. Imaging* **2007**, *34*, 2037.
9. (a) Foillard, S.; Jin, Z.; Garanger, E.; Boturyn, D.; Favrot, M.; Coll, J.-L.; Dumy, P. *ChemBioChem* **2008**, *9*, 2326; (b) Foillard, S.; Sancey, L.; Coll, J.-L.; Boturyn, D.; Dumy, P. *Org. Biomol. Chem.* **2009**, *7*, 221.
10. Sancey, L.; Garanger, E.; Foillard, S.; Schoehn, G.; Hurbin, A.; Albiges-Rizo, C.; Boturyn, D.; Souchier, C.; Grichine, A.; Dumy, P.; Coll, J.-L. *Mol. Ther.* **2009**, *17*, 837.
11. (a) Haubner, R.; Weber, W. A.; Beer, A. J.; Vabuliene, E.; Reim, D.; Sarbia, M.; Becker, K. F.; Goebel, M.; Hein, R.; Wester, H. J.; Kessler, H.; Schwaiger, M. *PLos Med.* **2005**, *2*, 244; (b) Zhang, X. Z.; Xiong, Z. M.; Wu, Y.; Cai, W. B.; Tseng, J. R.; Gambhir, S. S.; Chen, X. Y. *J. Nucl. Med.* **2006**, *47*, 113.
12. Foillard, S.; Olsten Rasmussen, M.; Razkin, J.; Boturyn, D.; Dumy, P. *J. Org. Chem.* **2008**, *73*, 983.
13. Boturyn, D.; Dumy, P. *Tetrahedron Lett.* **2001**, *42*, 2787.
14. Garanger, E.; Boturyn, D.; Jin, Z.; Dumy, P.; Favrot, M.-C.; Coll, J.-L. *Mol. Ther.* **2005**, *12*, 1168.
15. Jin, Z.; Josserand, V.; Razkin, J.; Garanger, E.; Boturyn, D.; Favrot, M.-C.; Dumy, P.; Coll, J.-L. *Mol. Imaging* **2006**, *5*, 188.
16. Keramidas, M.; Josserand, V.; Righini, C. A.; Wenk, C.; Faure, C.; Coll, J. L. *Br. J. Surg.* **2010**, *97*, 737.

JJCO Japanese Journal of Clinical Oncology 40th ANNIVERSARY

Jpn J Clin Oncol 2010;40(9)891–896
doi:10.1093/jjco/hyq099
Advance Access Publication 4 July 2010

Molecular Diagnosis of Multistage Hepatocarcinogenesis

Michiie Sakamoto*, Kathryn Effendi and Yohei Masugi

Department of Pathology, School of Medicine, Keio University, Tokyo, Japan

*For reprints and all correspondence: Michiie Sakamoto, Department of Pathology, School of Medicine, Keio University, 35 Shinanomachi, Shinjuku-ku, Tokyo 160-8582, Japan. E-mail: msakamot@sc.itc.keio.ac.jp

Received April 30, 2010; accepted May 22, 2010

Human hepatocellular carcinoma is recognized as a good model for multistage carcinogenesis, as the malignant steps from chronic liver disease through to advanced human hepatocellular carcinoma are relatively clear. We address the activation of different molecular pathways during hepatocarcinogenesis that is especially useful in the diagnosis of pathological multistage human hepatocellular carcinoma. In chronic liver disease, the gene-expression signature as well as the degree of liver fibrosis could help us to predict the development of human hepatocellular carcinoma or survival outcome after treatment for human hepatocellular carcinoma. Several genes, such as *HSP70*, *CAP2* and *GPC3*, have been identified as potential biomarkers for early human hepatocellular carcinoma. Classical oncogenes or tumor suppressor genes, such as *beta-catenin* and *p53*, are mutated during the progression from early to advanced human hepatocellular carcinoma. Also, the presence of hepatoblastic feature like CK19 in advanced human hepatocellular carcinoma can be used as a predictor of aggressive human hepatocellular carcinoma. Although many advances have been made in the diagnosis of multistage hepatocarcinogenesis, we still need further useful markers to more precisely evaluate each step of hepatocarcinogenesis for better treatment choices, and that will promote future molecular-targeted therapy.

Key words: chronic hepatitis – early HCC – advanced HCC – hepatocarcinogenesis – molecular markers

INTRODUCTION

Cancer is currently a major public health issue due to its high incidence and life-threatening nature. With careful and detailed follow-up of high-risk cases, we are now able to characterize and clarify the developmental process of human carcinogenesis, particularly in the early stages. In the case of human hepatocellular carcinoma (HCC), which still ranks as the third highest cause of cancer-related death globally (1), the malignant transformation step is well characterized. Through clinicopathological and molecular pathological observations, hepatocellular changes in HCC have been classified from chronic viral infection and liver cirrhosis, dysplastic nodules (DN) and early through to advanced HCC (Fig. 1). DN are usually found in chronic liver diseases and are classified as low grade or high grade (HGDN), depending on the degree of atypia. HGDN most often show increased cellularity, usually together with some cellular or structural atypia. However, these cellular or structural atypia are still indefinite for a diagnosis of HCC. In early HCC, the cell density increases compared with the surrounding non-cancerous background liver tissue, and there is an increased nuclear/cytoplasmic ratio. Although cytological atypia are still mild, abnormal trabecular or pseudoglandular patterns as well as various degrees of diffuse fatty changes are frequently observed. Tumor cells appear as small hepatocyte-like cells that merge imperceptibly with the surrounding hepatic parenchyma, and this is sometimes difficult to recognize, both grossly and microscopically. Recently, an international consensus was achieved, indicating that the presence of stromal invasion is an important feature of early HCC and differentiates early HCC from HGDN (2). The transitional progress from an early to more advanced stage is histologically described as a nodule-in-nodule lesion, where moderately or poorly differentiated cancerous tissue grows within a well-differentiated cancer nodule. Advanced HCC often shows intrahepatic metastasis spread through portal vein invasion.

Until now, many molecular mechanisms involved in multistep hepatocarcinogenesis have been reported. One of the prominent features of hepatocarcinogenesis is the increase in hypervascularity during the process of dedifferentiation and

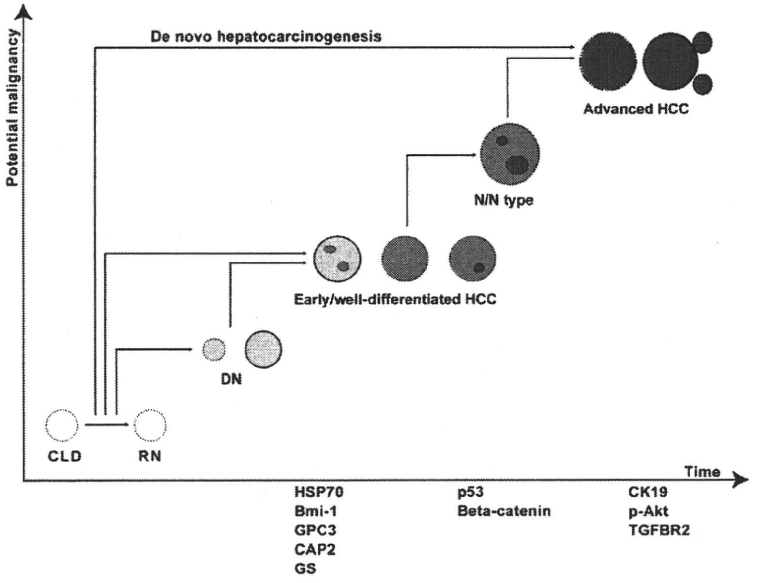

Figure 1. Evolution stage of human hepatocellular carcinoma (HCC) with its related molecular diagnosis. Some variable patterns may be observed in addition to the typical multistage developmental process of hepatocarcinogenesis. Some cases may show a direct development to the advanced stage of HCC, known as de novo hepatocarcinogenesis. CLD, chronic liver disease; RN, regenerative nodule; DN, dysplastic nodule; N/N, nodule-in-nodule.

progression, indicating the importance of angiogenic switches for the progression from early to progressed HCC (3). Understanding the molecular mechanisms involved in the malignant transformation of HCC is an important step to help us identify molecular markers or signatures in HCC development. However, the usefulness of these molecular markers in clinical practice needs careful evaluation. In this review, we will focus on the progress of some of the molecular pathology that has been, or could be, used in the diagnosis of multistage hepatocarcinogenesis.

RISK ASSESSMENT OF HCC DEVELOPMENT IN CHRONIC LIVER DISEASE

Hepatitis viral infection (hepatitis B virus (HBV), hepatitis C virus (HCV) or co-infection) is the most common cause for developing HCC worldwide. Almost all cases of HCC develop with the presence of chronic liver disease and if cirrhosis develops, the probability of HCC is increased. In HBV-infected individuals, the incidence of HCC is approximately 100 times higher compared with the uninfected population. HCV is still a major cause of HCC in Japan. HCV-associated HCC typically develops after 20–30 years after infection and is generally preceded by liver cirrhosis (4). Scoring the staging of chronic hepatitis obtained from liver biopsy specimens could be determined according to the internationally recognized degree of fibrosis scale (5). The risk of liver cancer development among individuals with HCV infection ranges between 1% and 7% per year. Another cytological change predictive for HCC development is steatosis, marked by clear vacuoles, due to fat accumulation within the hepatocytes. The presence of hepatic steatosis is associated with increased frequency of HCC in patients with HCV-related cirrhosis (6,7). In addition to these histological findings, identifying molecular changes in liver cirrhosis associated with HCC will be necessary for the proper management of chronic liver diseases and prevention of HCC. The genome-wide expression-profiling method has been widely applied as a new approach, not only to discover molecules involved in a variety of tumor carcinogenesis (8–10), but also to identify molecules associated with precancerous conditions (Fig. 2). Around 186 signature genes were reported to be associated with the risk for HCC recurrence and could predict the survival prognosis after resection of HCC, as well as identify compensated cirrhotic patients at a high risk for HCC development (11).

MOLECULAR DIAGNOSIS OF EARLY HCC

Early HCC is characterized as pre-invasive or early invasive cancer with a mild deviation of the clinicopathological features from chronic liver disease. Thus, early HCC lacks the typical findings of advanced HCC, such as increased arterial supply, elevated common tumor markers (α-fetoprotein (AFP), protein-induced by vitamin K absence or antagonist II (PIVKA II)) and obvious histological atypia. There have been several efforts to identify molecular signatures involved in early HCC, and some of them have been used as diagnostic markers. Heat shock protein 70 (*HSP70*), found by gene-expression profiling from approximately 12 600 analyzed genes, is abundantly upregulated in early HCC. Expression of *HSP70* increases under conditions of environmental cellular stress, thus the tumorigenesis process in early HCC may act as a stressful condition to stimulate *HSP70* expression (10). HSP70 expression is not observed in

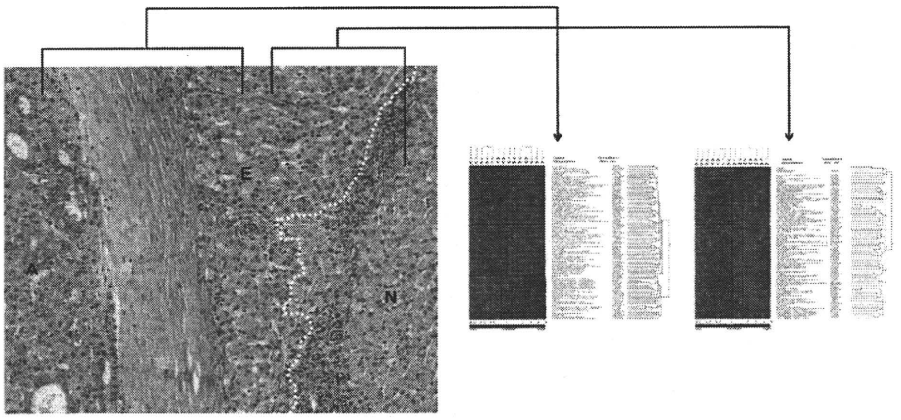

Figure 2. Two-way hierarchical clustering algorithm in multistep hepatocarcinogenesis. Comparison of expression profile between early HCC (E) components and their non-cancerous surrounding tissue (N), and between advanced HCC (A) and early HCC components. Using this method, we can identify upregulated and downregulated genes involved in multistep hepatocarcinogenesis.

non-malignant nodules or other benign nodular lesions, hepatocellular adenoma and focal nodular hyperplasia. This makes HSP70 a useful histological marker to distinguish early HCC from precancerous lesions and to differentiate benign and malignant liver nodules (12). Using the same profiling method, the cyclase-associated protein2 (*CAP2*) gene was also found to be upregulated in early HCC. *CAP* was originally identified in the budding yeast *Saccharomyces cerevisae*, and at least two isoforms of CAP, CAP1 and CAP2 have been found in mammals (13–15). Using our originally raised polyclonal antibody against human CAP2, we found that CAP2 was upregulated in a stepwise manner through the progression of HCC. Interestingly, stromal invasion, a characteristic feature of early HCC, was frequently found to be positive and clearly highlighted with CAP2 (16). Our unpublished observation also supports the evidence of CAP2 involvement in cancer cell invasion.

Other immunohistological markers commonly cited in early HCC are glypican-3 (GPC3) and glutamine synthetase (GS). GPC3 is a heparan sulfate proteoglycan anchored to the plasma membrane and normally expressed in the fetal liver and placenta, but not in normal adult liver tissue. GPC3 is widely recognized as an efficient serological and histochemical marker for early HCC (17–19). It is also reportedly helpful in distinguishing small focal lesions arising in liver cirrhosis and identifying some cirrhotic macronodules with malignant potential (20,21). However, GPC3 has also found to be expressed in benign liver tissue with active inflammation, which urges caution when interpreting GPC3 staining (22). Additional markers may thus be needed to boost the diagnosis. GS is an enzyme that catalyzes glutamate and ammonia to form glutamine in the mammalian liver (23). The final product from GS synthetase, glutamine, is reported to provide an energy source for tumor cells (24). GS is a target of the Wnt/beta-catenin pathway and is a good immunohistochemical marker of beta-catenin activation in HCC (25,26). Overexpression of GS increases with the stepwise progress of hepatocarcinogenesis, indicating an important role of GS in promoting the metastatic potential of HCC (27,28). A combination of the three-marker panel of HSP70, GPC3 and GS can raise the accuracy of detecting early HCC. A 72% sensitivity and 100% specificity, where the most sensitive combination was HSP70 and GPC3, have been shown (29).

Recently, we identified the overexpression of *Bmi-1*, a member of the Polycomb gene group, in early HCC. Bmi-1 is indicated as one of the signaling pathways that results in the 'stemness feature' in cancer through its ability to immortalize cells by inducing telomerase activity. *Bmi-1* also promotes tumorigenesis by acting as a negative regulator for the well-known tumor suppressors genes, *p16* and *p19* (30,31). In our study, Bmi-1 expression appeared as small dots inside the nuclear area that may reflect concentrated sites of Bmi-1 activity. Elevated Bmi-1 expression was particularly evident in early and well-differentiated HCC, compared with the surrounding, non-cancerous liver tissue (32). Investigations to explore the applicability of Bmi-1 as a new diagnostic marker for early HCC are currently on going.

MOLECULAR SUBCLASSIFICATION OF ADVANCED HCC

Advanced HCC shows a solid growth pattern with a decrease in the distinct trabecular pattern, and pleomorphisms are frequently observed. It commonly displays a variety of histological grading within its nodule; poorly differentiated tissue is located inside, surrounded by well-differentiated tissue. A transitional progress from early to advanced HCC is observed histologically as a nodule-in-nodule lesion. The presence of the *p53* mutation has been detected in the inner, advanced nodule, but not in the outer well surrounding nodule, suggesting an association between the *p53* gene mutation and the late events of HCC progression (33–35).

Nuclear accumulation of p53, detected by immunohistochemistry, is useful for the recognition of advanced HCC. Another mutation associated with the malignant progression of HCC is the *beta-catenin* mutation. Disruption of the Wnt/beta-catenin pathway causes accumulation of beta-catenin in the nucleus (36). However, the correlation of beta-catenin expression and HCC progression is not yet clear. Some studies report its association with a poor prognosis, whereas other studies associate it with a more favorable outcome (36–38). Additional signaling pathways associated with the aggressiveness of HCC include the TGF-β and Akt pathways. The potential of TGF-β gene expression to refine the diagnosis and prognostic predictions in HCC patients has also been reported. The outcome of TGF-β signaling is highly contextual in different tissues and depends on the cellular microenvironment. TGF-β signaling in carcinogenesis is intriguing due to its ability to act both as a tumor suppressor in the early stage, and a tumor promoter in the later stage. In HCC, changes in TGF-β signaling are still controversial and unclear. Coulouarn et al. showed that patients with a late TGF-β signature showed a significant decrease in mean survival time compared with patients with an early TGF-β signature. A late TGF-β signature predicted liver metastases and identified HCC cell lines according to their degree of invasiveness (39). We also found that poorly differentiated HCC showed a reduced expression of TGFBR2, and this correlated with intrahepatic metastasis and early recurrence (40). It will be interesting to further explore the implications of TGF-β signaling in HCC. Akt phosphorylation (p-Akt) has been identified as a significant risk factor for early disease recurrence and poor prognosis in HCC through its correlation with anchorage-independent growth malignant behavior (41).

In addition, some biliary or hepatic progenitor markers, such as CK7 or CK19, are frequently found in poorly differentiated cells (42). The prevalence of intrahepatic metastases was found to be significantly higher in patients with CK7-positive HCC, than in those with CK7-negative HCC. Patients with CK19 positivity had a significantly higher incidence of early recurrence suggesting a worse prognosis than CK19-negative HCC patients (42–45). HCC is postulated to be generated through carcinogenesis from hepatic progenitor cells (HPC) that are capable of differentiating into both hepatocytes and biliary epithelial cells (43,46). However, whether the hepatoblastic feature origin occurs via a de-differentiation progress, or originates from HPC, is still a matter of debate. Another hepatic progenitor cell marker, identified as epithelial cell adhesion molecule (EpCAM), when combined together with the embryonic liver marker, AFP, could help to define the clinicopathological characteristics of HCC subtypes. These HCC subtypes may resemble certain stages of hepatic lineages and enable prognostic assessment of HCC patients (47).

CONCLUSION

We have briefly reviewed the development and application of the molecular diagnosis of multistage hepatocarcinogenesis (Fig. 3). We need to standardize the histological

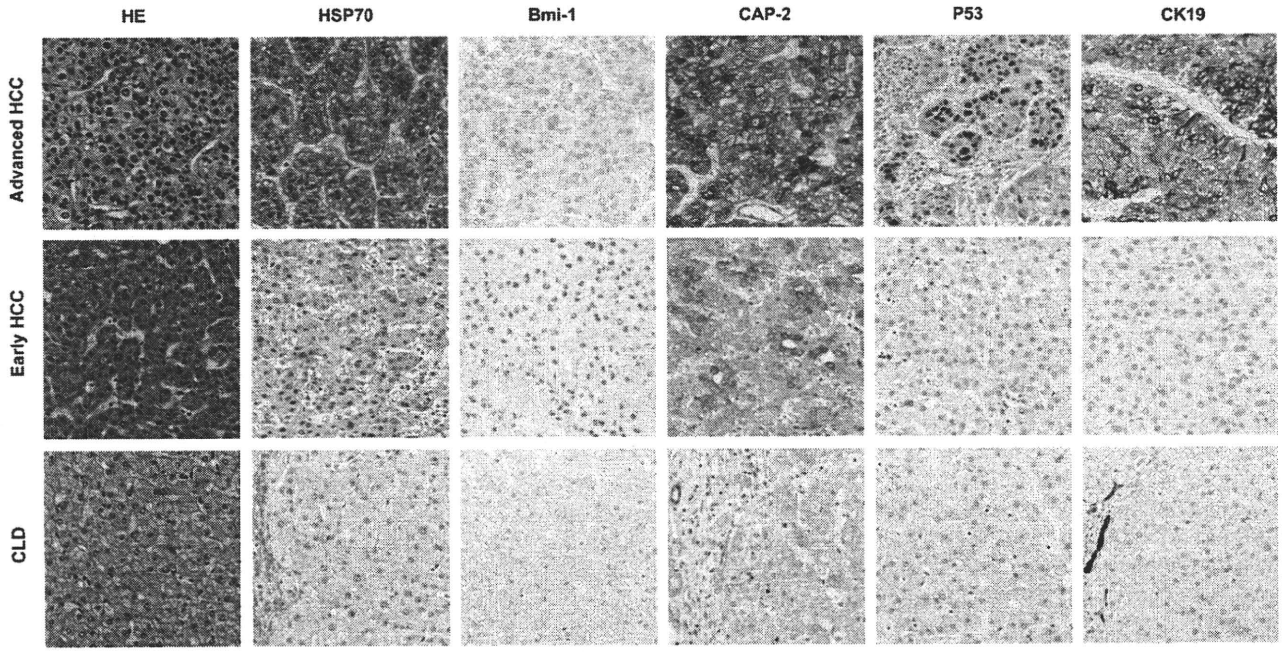

Figure 3. Panel of histological markers in HCC clinical specimens. The use of HSP70, Bmi-1 and CAP2 was helpful to recognize early stage of HCC. HSP70 and CAP2 expressions were getting increased following the progression of HCC, whereas Bmi-1 was particularly highly expressed in early- or well-differentiated HCC. In advanced stage of HCC, positive p53 and CK19 specimens were frequently observed. Their expressions were also related to a worse prognosis of HCC.

molecular markers used in the diagnosis of HCC, as the developmental process of hepatocarcinogenesis itself may not be simple and differs from patient to patient. We also need to detail the molecular characteristics and histological patterns that reflect the malignant potency in each step of hepatocarcinogenesis to determine the accurate staging of HCC. A combination diagnostic approach using biomarkers besides histological markers, such as serum markers, genetic markers or imaging contrast, will also greatly enhance our ability to overcome the highly malignant HCC. This will further establish prevention, as well as promote better treatment choice in the new era of molecular-targeted therapy and individualized cancer treatment.

Conflict of interest statement

None declared.

References

1. Parkin DM, Bray F, Ferlay J, Pisani P. Global cancer statistics, 2002. *CA Cancer J Clin* 2005;55:74–108.
2. Pathologic diagnosis of early hepatocellular carcinoma: a report of the international consensus group for hepatocellular neoplasia. *Hepatology* 2009;49:658–64.
3. Sugimachi K, Tanaka S, Terashi T, Taguchi K, Rikimaru T, Sugimachi K. The mechanisms of angiogenesis in hepatocellular carcinoma: angiogenic switch during tumor progression. *Surgery* 2002;131:S135–41.
4. Hirohashi S, Ishak KG, Kojiro M, Puig PL, Wanless IR, Fischer HP, et al. Hepatocellular carcinoma. In: Hamilton SR, Aaltonen LA editors. *Pathology and Genetics of Tumours of the Digestive System.* Lyon: IARC Press, 2000;159–72.
5. Desmet VJ, Gerber M, Hoofnagle JH, Manns M, Scheuer PJ. Classification of chronic hepatitis: diagnosis, grading and staging. *Hepatology* 1994;19:1513–20.
6. Pekow JR, Bhan AK, Zheng H, Chung RT. Hepatic steatosis is associated with increased frequency of hepatocellular carcinoma in patients with hepatitis C-related cirrhosis. *Cancer* 2007;109:2490–6.
7. Hourigan LF, Macdonald GA, Purdie D, Whitehall VH, Shorthouse C, Clouston A, et al. Fibrosis in chronic hepatitis C correlates significantly with body mass index and steatosis. *Hepatology* 1999;29:1215–9.
8. Golub TR, Slonim DK, Tamayo P, Huard C, Gaasenbeek M, Mesirov JP, et al. Molecular classification of cancer: class discovery and class prediction by gene expression monitoring. *Science* 1999; 286:531–7.
9. Bittner M, Meltzer P, Chen Y, Jiang Y, Seftor E, Hendrix M, et al. Molecular classification of cutaneous malignant melanoma by gene expression profiling. *Nature* 2000;406:536–40.
10. Chuma M, Sakamoto M, Yamazaki K, Ohta T, Ohki M, Asaka M, et al. Expression profiling in multistage hepatocarcinogenesis: identification of HSP70 as a molecular marker of early hepatocellular carcinoma. *Hepatology* 2003;37:198–207.
11. Hoshida Y, Villanueva A, Kobayashi M, Peix J, Chiang DY, Camargo A, et al. Gene expression in fixed tissues and outcome in hepatocellular carcinoma. *N Engl J Med* 2008;359:1995–2004.
12. Sakamoto M. Early HCC: diagnosis and molecular markers. *J Gastroenterol* 2009;44(Suppl 19):108–11.
13. Fedor-Chaiken M, Deschenes RJ, Broach JR. SRV2, a gene required for RAS activation of adenylate cyclase in yeast. *Cell* 1990;61:329–40.
14. Yu G, Swiston J, Young D. Comparison of human CAP and CAP2, homologs of the yeast adenylyl cyclase-associated proteins. *J Cell Sci* 1994;107:1671–8.
15. Swiston J, Hubberstey A, Yu G, Young D. Differential expression of CAP and CAP2 in adult rat tissues. *Gene* 1995;165:273–7.
16. Shibata R, Mori T, Du W, Chuma M, Gotoh M, Shimazu M, et al. Overexpression of cyclase-associated protein 2 in multistage hepatocarcinogenesis. *Clin Cancer Res* 2006;12:5363–8.
17. Capurro M, Wanless IR, Sherman M, Deboer G, Shi W, Miyoshi E, et al. Glypican-3: a novel serum and histochemical marker for hepatocellular carcinoma. *Gastroenterology* 2003;125:89–97.
18. Nakatsura T, Yoshitake Y, Senju S, Monji M, Komori H, Motomura Y, et al. Glypican-3, overexpressed specifically in human hepatocellular carcinoma, is a novel tumor marker. *Biochem Biophys Res Commun* 2003;306:16–25.
19. Hippo Y, Watanabe K, Watanabe A, Midorikawa Y, Yamamoto S, Ihara S, et al. Identification of soluble NH2-terminal fragment of glypican-3 as a serological marker for early-stage hepatocellular carcinoma. *Cancer Res* 2004;64:2418–23.
20. Libbrecht L, Severi T, Cassiman D, Vander Borght S, Pirenne J, Nevens F, et al. Glypican-3 expression distinguishes small hepatocellular carcinomas from cirrhosis, dysplastic nodules, and focal nodular hyperplasia-like nodules. *Am J Surg Pathol* 2006;30:1405–11.
21. Wang XY, Degos F, Dubois S, Tessiore S, Allegretta M, Guttmann RD, et al. Glypican-3 expression in hepatocellular tumors: diagnostic value for preneoplastic lesions and hepatocellular carcinomas. *Hum Pathol* 2006;37:1435–41.
22. Abdul-Al HM, Makhlouf HR, Wang G, Goodman ZD. Glypican-3 expression in benign liver tissue with active hepatitis C: implications for the diagnosis of hepatocellular carcinoma. *Hum Pathol* 2008; 39:209–12.
23. Haussinger D, Sies H, Gerok W. Functional hepatocyte heterogeneity in ammonia metabolism. The intercellular glutamine cycle. *J Hepatol* 1985;1:3–14.
24. Reitzer LJ, Wice BM, Kennell D. Evidence that glutamine, not sugar, is the major energy source for cultured HeLa cells. *J Biol Chem* 1979;254:2669–76.
25. Cadoret A, Ovejero C, Terris B, Souil E, Levy L, Lamers WH, et al. New targets of beta-catenin signaling in the liver are involved in the glutamine metabolism. *Oncogene* 2002;21:8293–301.
26. Zucman-Rossi J, Benhamouche S, Godard C, Boyault S, Grimber G, Balabaud C, et al. Differential effects of inactivated Axin1 and activated beta-catenin mutations in human hepatocellular carcinomas. *Oncogene* 2007;26:774–80.
27. Christa L, Simon MT, Flinois JP, Gebhardt R, Brechot C, Lasserre C. Overexpression of glutamine synthetase in human primary liver cancer. *Gastroenterology* 1994;106:1312–20.
28. Osada T, Sakamoto M, Nagawa H, Yamamoto J, Matsuno Y, Iwamatsu A, et al. Acquisition of glutamine synthetase expression in human hepatocarcinogenesis: relation to disease recurrence and possible regulation by ubiquitin-dependent proteolysis. *Cancer* 1999;85:819–31.
29. DiTommaso L, Franchi G, Park YN, Fiamengo B, Destro A, Morenghi E, et al. Diagnostic value of HSP70, glypican 3, and glutamine synthetase in hepatocellular nodules in cirrhosis. *Hepatology* 2007;45:725–34.
30. Valk-Lingbeek ME, Bruggeman SW, van Lohuizen M. Stem cells and cancer; the polycomb connection. *Cell* 2004;118:409–18.
31. Dimri GP, Martinez JL, Jacobs JJ, Keblusek P, Itahana K, Van Lohuizen M, et al. The Bmi-1 oncogene induces telomerase activity and immortalizes human mammary epithelial cells. *Cancer Res* 2002;62:4736–45.
32. Effendi K, Mori T, Komuta M, Masugi Y, Du W, Sakamoto M. Bmi-1 gene is upregulated in early-stage hepatocellular carcinoma and correlates with ATP-binding cassette transporter B1 expression. *Cancer Sci* 2010;101:666–72.
33. Oda T, Tsuda H, Sakamoto M, Hirohashi S. Different mutations of the p53 gene in nodule-in-nodule hepatocellular carcinoma as a evidence for multistage progression. *Cancer Lett* 1994;83:197–200.
34. Oda T, Tsuda H, Scarpa A, Sakamoto M, Hirohashi S. p53 gene mutation spectrum in hepatocellular carcinoma. *Cancer Res* 1992;52:6358–64.
35. Oda T, Tsuda H, Scarpa A, Sakamoto M, Hirohashi S. Mutation pattern of the p53 gene as a diagnostic marker for multiple hepatocellular carcinoma. *Cancer Res* 1992;52:3674–8.
36. Kondo Y, Kanai Y, Sakamoto M, Genda T, Mizokami M, Ueda R, et al. Beta-catenin accumulation and mutation of exon 3 of the beta-catenin gene in hepatocellular carcinoma. *Jpn J Cancer Res* 1999;90:1301–9.

37. Endo K, Ueda T, Ueyama J, Ohta T, Terada T. Immunoreactive E-cadherin, alpha-catenin, beta-catenin, and gamma-catenin proteins in hepatocellular carcinoma: relationships with tumor grade, clinicopathologic parameters, and patients' survival. *Hum Pathol* 2000;31:558–65.
38. Mao TL, Chu JS, Jeng YM, Lai PL, Hsu HC. Expression of mutant nuclear beta-catenin correlates with non-invasive hepatocellular carcinoma, absence of portal vein spread, and good prognosis. *J Pathol* 2001;193:95–101.
39. Coulouarn C, Factor VM, Thorgeirsson SS. Transforming growth factor-beta gene expression signature in mouse hepatocytes predicts clinical outcome in human cancer. *Hepatology* 2008;47: 2059–67.
40. Mamiya T, Yamazaki K, Masugi Y, Mori T, Effendi K, Du W, et al. Reduced transforming growth factor-beta receptor II expression in hepatocellular carcinoma correlates with intrahepatic metastasis. *Lab Invest* 2010 June 7. [Epub ahead of print].
41. Nakanishi K, Sakamoto M, Yamasaki S, Todo S, Hirohashi S. Akt phosphorylation is a risk factor for early disease recurrence and poor prognosis in hepatocellular carcinoma. *Cancer* 2005;103:307–12.
42. Uenishi T, Kubo S, Yamamoto T, Shuto T, Ogawa M, Tanaka H, et al. Cytokeratin 19 expression in hepatocellular carcinoma predicts early postoperative recurrence. *Cancer Sci* 2003;94:851–7.
43. Wu PC, Fang JW, Lau VK, Lai CL, Lo CK, Lau JY. Classification of hepatocellular carcinoma according to hepatocellular and biliary differentiation markers. Clinical and biological implications. *Am J Pathol* 1996;149:1167–75.
44. Yamamoto T, Uenishi T, Ogawa M, Ichikawa T, Hai S, Sakabe K, et al. Immunohistologic attempt to find carcinogenesis from hepatic progenitor cell in hepatocellular carcinoma. *Dig Surg* 2005;22:364–70.
45. Durnez A, Verslype C, Nevens F, Fevery J, Aerts R, Pirenne J, et al. The clinicopathological and prognostic relevance of cytokeratin 7 and 19 expression in hepatocellular carcinoma. A possible progenitor cell origin. *Histopathology* 2006;49:138–51.
46. Lee JS, Heo J, Libbrecht L, Chu IS, Kaposi-Novak P, Calvisi DF, et al. A novel prognostic subtype of human hepatocellular carcinoma derived from hepatic progenitor cells. *Nat Med* 2006;12:410–6.
47. Yamashita T, Forgues M, Wang W, Kim JW, Ye Q, Jia H, et al. EpCAM and alpha-fetoprotein expression defines novel prognostic subtypes of hepatocellular carcinoma. *Cancer Res* 2008;68:1451–61.

Laboratory Investigation (2010) 90, 1339–1345

Reduced transforming growth factor-β receptor II expression in hepatocellular carcinoma correlates with intrahepatic metastasis

Takao Mamiya[1,2,4], Ken Yamazaki[1,4], Yohei Masugi[1], Taisuke Mori[1], Kathryn Effendi[1], Wenlin Du[1], Taizo Hibi[3], Minoru Tanabe[3], Masakazu Ueda[3], Tadatoshi Takayama[2] and Michiie Sakamoto[1]

Hepatocellular carcinoma (HCC) occurs mainly in the liver associated with chronic hepatitis and hepatic cirrhosis as a result of prolonged viral infection. Transforming growth factor-β (TGF-β) induces the fibrosis in hepatic cirrhosis, although it is also an inhibitor of hepatocyte proliferation. To understand the role of TGF-β signaling in HCC progression, we analyzed gene expression in HCC cells in relation to TGF-β signaling using a two-way clustering algorithm. By the analysis, five HCC cell lines were classified into two groups according to their metastatic capacity. TGF-β receptor II (TGFBR2) was downregulated in metastatic cells, which did not show a response to TGF-β. Immunohistochemistry demonstrated clear membrane distribution of TGFBR2 in noncancerous hepatocytes, whereas reduced TGFBR2 expression was observed in 34 of 136 HCCs. In clinical cases, reduced TGFBR2 expression correlated with larger tumor size ($P<0.001$), poor differentiation ($P<0.001$), portal vein invasion ($P=0.002$), intrahepatic metastasis (IM) ($P<0.001$), and shorter recurrence-free survival ($P=0.022$). In conclusion, reduced TGFBR2 expression was associated with aggressive features of HCC such as IM, and may represent an immunohistochemical biomarker to detect aggressive HCC.
Laboratory Investigation (2010) **90,** 1339–1345; doi:10.1038/labinvest.2010.105; published online 7 June 2010

KEYWORDS: biomarker; HCC; immunohistochemistry; IM; TGF-β receptor II

Hepatocellular carcinoma (HCC) is a common cause of death from cancer worldwide.[1] Prolonged infection with hepatitis virus often causes chronic hepatitis, followed by liver cirrhosis.[2] During the development of these liver diseases, transforming growth factor-β (TGF-β) has an important role in fibrosis of the lesions.[3] HCCs mainly occur in those injured livers with activated TGF-β signaling, although TGF-β inhibits hepatocyte cell growth in the normal liver.[4,5]

TGF-β signaling is activated when a TGF-β ligand binds to its receptor on the cell membrane. The downstream effectors, SMAD2 and SMAD3, together with SMAD4, translocate to the nucleus and regulate the expression of various genes, including cyclin-dependent kinase inhibitor 1A (*CDKN1A*), which is involved in cell growth arrest.[6,7] TGF-β signaling is also suggested to be involved in the malignant progression of tumors. TGF-β can induce epithelial–mesenchymal transition and promote tumor cell invasion, and may also have angiogenic and immunosuppressive effects on the tumor microenvironment, all of which promote metastasis.[8]

Mutations in the TGF-β superfamily genes have been found in various cancers. The TGF-β receptor II (*TGFBR2*) gene is frequently mutated in colon cancers,[9,10] gastric cancers,[10,11] and in gliomas[12] with microsatellite instability. *SMAD4* mutations occur mainly in pancreatic cancers, in which the *SMAD4* gene was first identified as a tumor-suppressor gene.[13] In HCCs, however, mutations in TGF-β superfamily genes are rare,[14,15] and alteration of TGF-β signaling is still unclear and controversial. To investigate alterations of TGF-β signaling in HCC progression, we compared the expression profiles of TGF-β signaling-related genes in HCC cells exhibiting different metastatic potential. We also investigated TGFBR2 expression in HCC cells.

[1]Department of Pathology, School of Medicine, Keio University, Tokyo, Japan; [2]Department of Digestive Surgery, Nihon University School of Medicine, Tokyo, Japan and [3]Department of Surgery, School of Medicine, Keio University, Tokyo, Japan
Correspondence: Dr M Sakamoto, MD, PhD, Department of Pathology, School of Medicine, Keio University, 35 Shinanomachi, Shinjuku-ku, Tokyo 160-8582, Japan.
E-mail: msakamot@sc.itc.keio.ac.jp
[4]These authors contributed equally to this work.

Received 28 November 2009; revised 25 March 2010; accepted 13 April 2010

MATERIALS AND METHODS

Clinical Specimens of HCC

HCCs and corresponding, noncancerous liver tissue were obtained from patients who underwent surgical resection at the Keio University Hospital, Japan. We analyzed 136 nodules resected from 92 patients, including 12 patients with multicentric HCC. A histological diagnosis of HCC was made according to the WHO criteria.[16] The diagnosis of tumor recurrence was based on radiological findings and tumor markers in the serum. Time to recurrence was calculated as the period from the date of surgery until recurrence. This study was approved by the Ethics Committee of Keio University.

Cell Culture and TGF-β Treatment

The human HCC cell lines, PLC/PRF/5 and Hep G2, were obtained from the American Type Culture Collection (Manassas, VA, USA). KIM-1, KYN-2, and Li7 were established as previously reported.[17–19] All the cells were grown in RPMI 1640 (Sigma-Aldrich, St Louis, MO, USA) medium supplemented with 10% fetal bovine serum (FBS), 100 U/ml penicillin, and 100 μg/ml streptomycin. For treatment of PLC/PRF/5 and Li7 cells with TGF-β, the cells were cultured in RPMI 1640 medium supplemented with 5 ng/ml TGF-β1 (PeproTech EC, London, UK) and 0.5% FBS.

Hierarchical Clustering

Gene-expression profiles of TGF-β-related genes in PLC/PRF/5, Hep G2, KIM-1, KYN-2, and Li7 cells were clustered using established algorithms implemented in the software program, Cluster.[20] Centroid linkage clustering with uncentered correlation was used. TreeView software (http://rana.lbl.gov/EisenSoftware.htm) generated a visual representation of clusters. Microarray data are available at Genome Medicine Database of Japan (https://gemdbj.nibio.go.jp/dgdb/).

Western Blot

PLC/PRF/5, Hep G2, KIM-1, KYN-2, and Li7 cells were lysed in lysis buffer (0.1% SDS, 1% Nonidet P-40, 150 mM NaCl, 50 mM Tris–HCl (pH 7.5), 5 mM EDTA) supplemented with Complete Protease Inhibitor Cocktail (Roche Molecular Biochemicals, Mannheim, Germany). The lysates were separated by electrophoresis on NuPAGE 4–12% Bis–Tris gels (Invitrogen, Carlsbad, CA, USA), and transferred to PVDF membrane according to the manufacturer's instructions. The blotted membrane was probed with a rabbit TGFBR2 antibody (Upstate, Lake Placid, NY, USA) and bound antibody was detected with ECL Western blotting detection reagents (GE Healthcare, Uppsala, Sweden).

Semiquantitative RT-PCR

Total RNA was purified using the RNeasy Mini Kit (Qiagen, Valencia, CA, USA). Single-stranded cDNA was synthesized from 1 μg of total RNA using the oligo (dT) primer and M-MLV reverse transcriptase (Promega, Madison, WI, USA) at 42°C for 1 h. Primers and PCR cycles were as follows: SERPINE1 (sense, 5′-TCCTGGTTCTGCCCAAGTTCTC-3′; antisense, 5′-CACAAAGAGGAAGGGTCTGTCCA-3′, 30 cycles), and GAPDH (sense, 5′-AAGGTCATCCCTGAGCT GAACG-3′; antisense, 5′-CAAAGGTGGAGGAGTGGGTGTC-3′, 23 cycles). PCR products were separated by agarose gel electrophoresis and detected by staining with ethidium bromide.

Cell Proliferation Assay

In 24-well plates, three wells each of PLC/PRF/5 and Li7 cells were treated with, or without, TGF-β for 3 days. After 0, 1, 2, and 3 days of treatment, the culture medium was replaced with 10% WST-1 reagent (Roche Molecular Biochemicals) in 10% FBS/RPMI 1640, and incubated for 30 min at 37°C. The absorbance of the converted dye was measured at a wavelength of 450 nm, with background subtraction at 630 nm, using a Bio-Rad Model 550 microplate reader (Bio-Rad Laboratories, Hercules, CA, USA). Results were expressed as the ratio of viable cells relative to those on day 0.

IHC

Formalin-fixed, paraffin-embedded tissue sections were boiled for 30 min in 10 mmol/l Tris–HCl (pH 9.0), 150 mM NaCl for antigen retrieval, and labeled with rabbit polyclonal antibody against TGFBR2 (1:200) (Upstate) overnight at 4°C. Bound antibody was visualized using a peroxidase-conjugated secondary antibody (ImmPRESS, Vector Laboratories, Burlingame, CA, USA), and color developed with diaminobenzidine. After counterstaining with hematoxylin, sections were mounted on coverslips.

Statistical Analysis

The χ^2-test was used when appropriate to determine the correlations between clinicopathological variables and TGFBR2 expression. Cumulative recurrence rate was calculated with the Kaplan–Meier method, and the log-rank test was applied to compare survival between different groups. In 92 consecutive patients who underwent surgery for HCC from 2003 through 2006, 12 patients of the liver transplantation were excluded from the analysis of recurrence-free analysis. All statistical analyses were carried out using SPSS statistical software (SPSS, Chicago, IL, USA).

RESULTS

TGF-β Superfamily Genes in HCC Cells

To understand the expression levels of TGF-β signaling-related genes, expression profiles of HCC cells were examined by two-way clustering analysis. In 12 625 probes on a Gene Chip HG-U95A array, 93 probes targeting 56 genes were selected based on Gene Ontology annotation terms, including 'transforming growth factor beta.' Five HCC cell lines were roughly classified into two clusters, one of which involved PLC/PRF/5, Hep G2, and KIM-1 cells, and another,

KYN-2 and Li7 cells (Figure 1). These cells have been previously classified into two groups on the basis of metastatic potential in a mouse intrahepatic metastasis (IM) model, in which orthotopically implanted KYN-2 and Li7 cells formed secondary foci in the mouse liver, whereas others did not.[21] Thus, the classification by the clustering analysis in this study reflected the classification based on metastatic potential in the mouse model. In the central transducers of TGF-β signaling pathway (ligands–receptors–SMADs), *TGFBR2* showed markedly different expression between the two groups. Mutations of the *TGFBR2* gene frequently found in some cancers have not been identified in HCC; therefore, we speculated whether the reduced expression level of *TGFBR2* causes suppression of TGF-β signaling without mutations, and selected it for further analyses. Although *TGFBR2* expression was downregulated in metastatic (KYN-2 and Li7) cells, not all the TGF-β-responsive gene expression correlated with *TGFBR2* expression levels. This suggests that heterogeneous TGF-β responses may be reflected in the expression signature.

The differential expression of TGFBR2 in the HCC cell lines was confirmed by RT-PCR (Supplementary Figure 1a) and Western blot analyses (Figure 2a). Compared with the nonmetastatic cells, TGFBR2 expression was reduced in the metastatic cells. Thus, TGFBR2 was downregulated at both the mRNA and protein level. Expression levels of TGF-β receptor I (TGFBR1), a binding partner of TGFBR2, were almost same in these cell lines (Supplementary Figure 1a).

Response to TGF-β in HCC Cells

To examine the functional role of the differential expression of TGFBR2, the response to TGF-β in HCC cells was assayed by semiquantitative RT-PCR (Figure 2b). After 3 h of treatment with 5 ng/ml TGF-β1, there was elevated expression of a TGF-β-inducible gene, *SERPINE1* (plasminogen activator inhibitor type 1), in the nonmetastatic cells. In contrast, *SERPINE1* expression was not detected in either the KYN-2 or the Li7 cells, before and after treatment. Similarly, another TGF-β-responsive gene, *SMAD7*, was upregulated in PLC/PRF/5 cells by TGF-β stimulation, but not in the Li7 cells (Supplementary Figure 1b).

We also evaluated the proliferative response of PLC/PRF/5 and Li7 cells to TGF-β. As shown in Figure 2c, proliferation of PLC/PRF/5 cells was reduced by treatment with TGF-β, whereas Li7 cells showed no significant difference. Upregulated expression of *CDKN1A* was observed in PLC/PRF/5 cells after TGF-β addition, but not in the Li7 cells (Supplementary Figure 1b). These results suggest that the growth arrest mediated by CDKN1A through TGF-β signaling is dependent on the expression level of TGFBR2.

TGFBR2 Expression in HCCs

Expression levels of TGFBR2 in clinical cases of HCC were examined by immunohistochemistry (IHC). To optimize the conditions for IHC, sections of tumors formed in

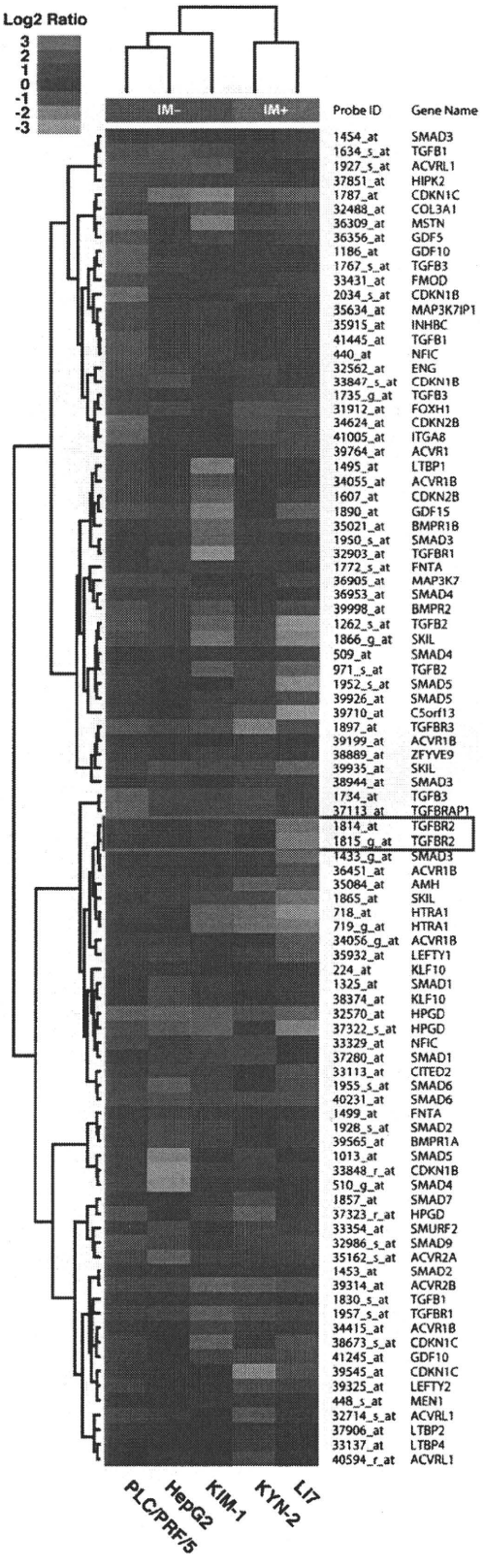

Figure 1 Two-way clustering of TGF-β signaling-related genes in five HCC cell lines. The vertical axis corresponds to cells, and the horizontal axis to genes. Gene expression levels are presented by log(2) ratio to mean intensity, and depicted as color variation from red (high expression) to green (low expression).

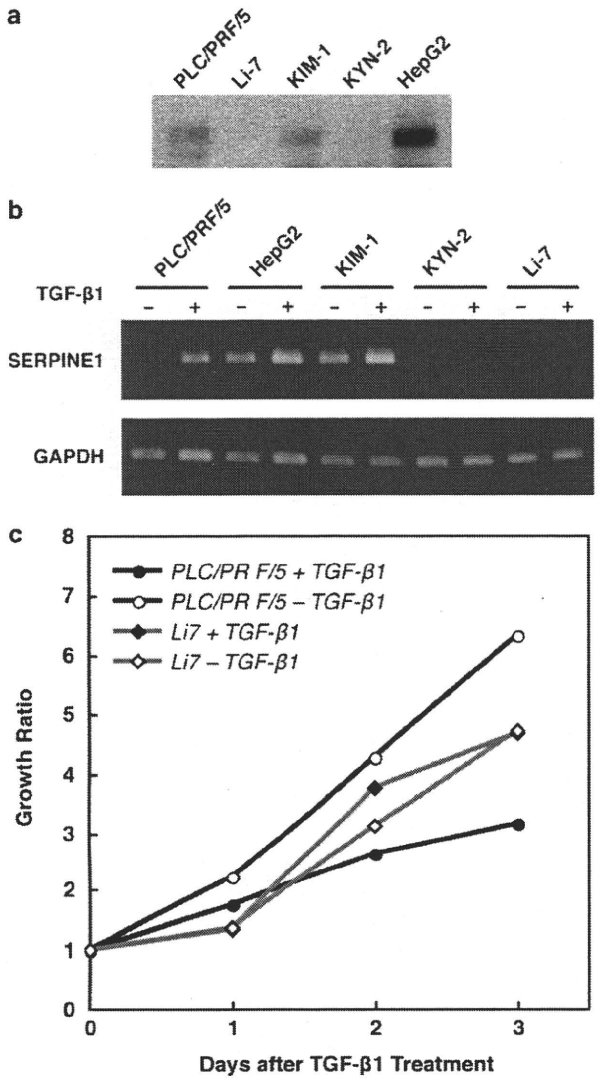

Figure 2 TGFBR2 expression and response of hepatocellular carcinoma cells to TGF-β. (**a**) Western blot analysis shows a reduction of TGFBR2 expression in the KYN-2 and Li7 cells, compared with the others. Equal protein loading was confirmed by staining the blot with amido black (data not shown). (**b**) RT-PCR shows no response of KYN-2 and Li7 cells to TGF-β. Following treatment with (+), or without (−), TGF-β, expression of *SERPINE1* was upregulated in PLC/PRF/5, Hep G2, and KIM-1 cells. (**c**) Cell proliferation assays in PLC/PRF/5 and Li7 cells treated with, or without, TGF-β, for 3 days. The growth ratio indicates the relative cell number compared with that of day 0 in each series.

immunodeficient mice by subcutaneous inoculation of PLC/PRF/5 or Li7 cells were prepared. By boiling the sections for 30 min in 10 mmol/l Tris–HCl buffer (pH 9.0), TGFBR2 could be successfully detected in the cell membrane of PLC/PRF/5 cells, but not in the Li7 cells (Supplementary Figure 2). We performed IHC on 136 nodules of human HCC specimens using these optimal conditions. TGFBR2 was detected in noncancerous hepatocytes, especially on the cell membrane and corresponding to the expected localization for a membrane receptor (Figure 3). Bile duct cells and vascular endothelial cells also expressed TGFBR2 (Figure 3a; an asterisk and arrowheads, respectively). Staining levels in each cell type were basically homogenous. On the other hand, the expression level of TGFBR2 in cancer cells varied among nodules. Compared with noncancerous hepatocytes, unchanged expression of TGFBR2 was found in some nodules (Figure 3b), whereas reduced expression was seen in others (Figure 3c). From the total of 136 nodules examined, reduced expression ($\geq$ 10% of tumor cells showing no membranous staining of TGFBR2) was observed in 34 nodules, and expression levels similar to that observed in the noncancerous hepatocytes was observed in 102 nodules (Table 1). Poorly differentiated cells frequently showed reduced expression of TGFBR2. In the cells that formed a tumor embolus (Figure 3d), TGFBR2 expression was significantly reduced compared with adjacent hepatocytes, and there was no membrane localization of TGFBR2. The results of IHC analyses from clinical patient samples demonstrate that reduced expression of TGFBR2 correlated with poor differentiation, portal vein invasion, and IM.

During a median follow-up of 26 months (range, 0–67 months), the time-to-recurrence was analyzed in 80 cases with HCC. Log-rank analysis showed that patients with reduced TGFBR2 expression had a significantly shorter time-to-recurrence ($P = 0.022$), compared with patients with TGFBR2 expression level similar to the adjacent hepatocyte (Figure 4). Expression levels of TGFBR2 were different among foci of multicentric HCCs. Therefore, patients with at least one focus showing reduced TGFBR2 expression were classified into the reduced TGFBR2 group.

DISCUSSION

TGFBR2 is a major TGF-β signaling molecule often found to be one of the genes altered in cancer. Its expression levels in HCC have been controversial and its biological role in HCC remains unclarified. Some reports show unchanged TGFBR2 expression in HCC compared with adjacent liver tissue,[22] whereas others show downregulation in 50[23] and 60%[24] of HCCs. We found differential expression of TGFBR2 between metastatic and nonmetastatic HCC cells, and, with IHC, demonstrated reduced expression of TGFBR2 in 25% of HCC cases. TGFBR2 shows a clear membrane distribution in noncancerous hepatocytes and this can be useful when using IHC to assess specific downregulation in HCC. Although the mechanism of TGFBR2 downregulation in HCC remains unknown, microarray and RT-PCR analyses show that *TGFBR2* gene expression is reduced at the mRNA level. Epigenetic silencing of *TGFBR2* by promoter methylation occurs in stomach, lung, and prostate cancers.[25–27] Considering that mutations or loss of the *TGFBR2* gene are rare in HCCs, epigenetic silencing may be involved in reduced *TGFBR2* expression in HCC.

Progression of HCC often leads to vascular invasion and IM, which correlate with recurrence after treatment, and

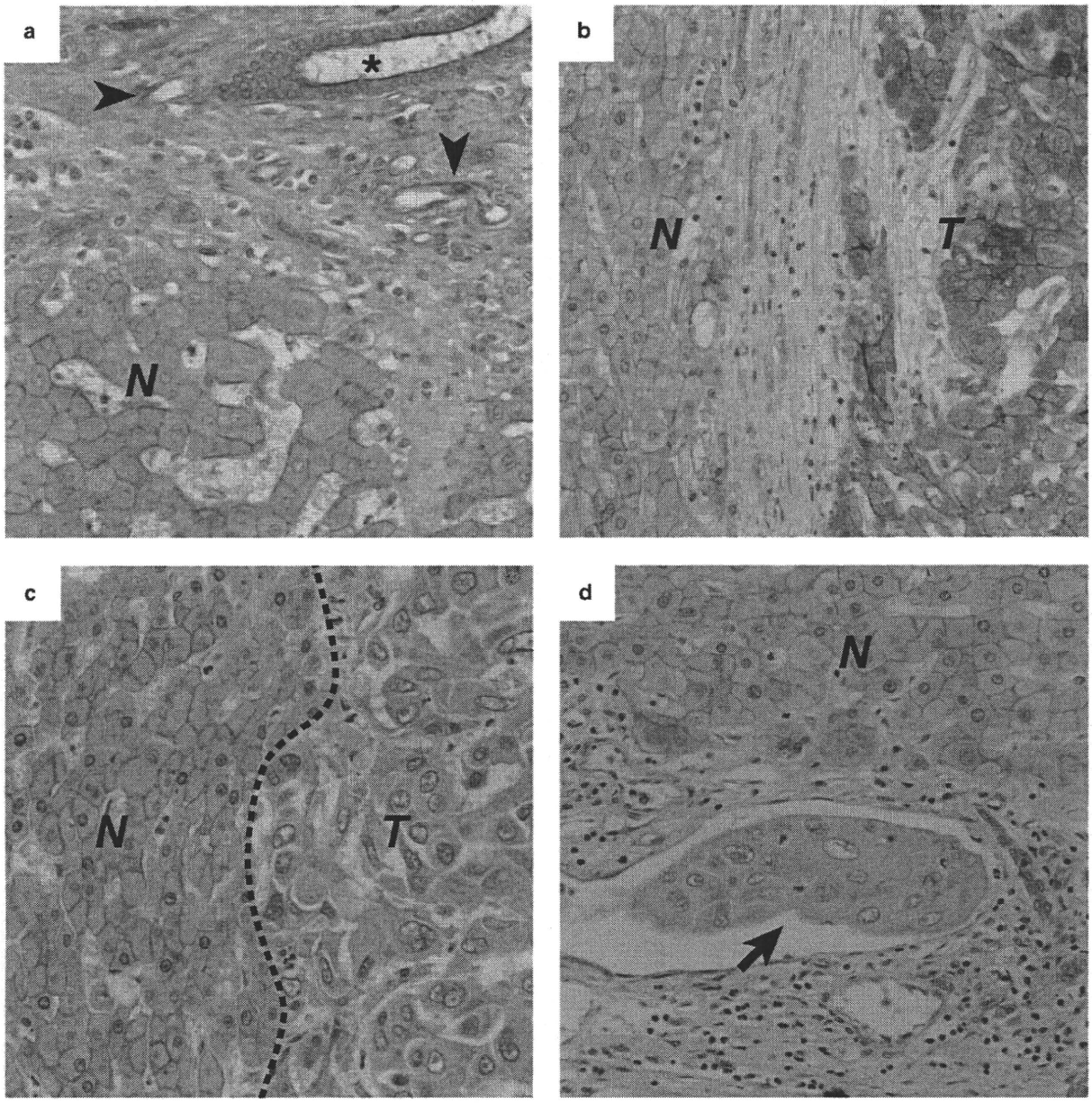

Figure 3 Immunolabeling of TGFBR2 in clinical specimens of HCC. (**a**) Nonneoplastic hepatocytes (*N*), bile duct epithelial cells (asterisk), and vascular endothelial cells (arrowheads) showed TGFBR2 immunoreactivity on the cell membrane. Unchanged (**b**), or reduced (**c**) expression of TGFBR2 was shown in tumor cells (*T*), compared with hepatocytes (*N*). (**d**) Tumor cells forming an embolus showed reduced TGFBR2 expression (arrow) compared with adjacent hepatocytes (*N*).

poor prognosis.[28,29] IM is thought to develop through tumor cell dissemination through the portal vein.[30] Previous studies using the mouse IM model indicate activation of RhoA[21] and AKT,[31] and overexpression of cortactin[32] in metastatic HCC cells. We showed that the expression signature of TGF-β signaling-related genes classified the HCC cells into two groups according to their metastatic potential. Reduced TGFBR2 expression significantly correlated with the aggressive features of HCC. The results suggest that TGF-β signaling has a suppressive role in HCC progression, as downregulated TGFBR2 appears to result in impaired TGF-β signaling. However, TGF-β signaling in HCC is complicated. Giannelli and coworkers[33–35] demonstrated the involvement of TGF-β signaling in promoting HCC growth, progression, and metastasis, and Coulouarn *et al*[36] showed that the expression signature of the late TGF-β response predicts liver metastasis and poor outcome in HCC patients. Considering these findings, TGF-β signaling may not be

Table 1 Correlations between clinicopathological characteristics and TGFBR2 expression in patients with HCC

Characteristics	TGFBR2 expression		
	Unchanged ($n = 102$)	Reduced ($n = 34$)	χ^2 test P value
Mean age (± s.d.)	62.2 ± 9.4	60.2 ± 12.8	0.421[a]
Gender			0.475
Male	89	28	
Female	13	6	
Etiology			0.023
HBV	17	13	
HCV	68	15	
NBNC	16	6	
AFP serum level (ng/ml)			0.202
<20	34	13	
≥20	25	17	
Tumor size (cm)			<0.001
≤2	54	6	
>2	48	28	
Differentiation			<0.001
Well	34	2	
Moderately	62	18	
Poorly	6	14	
Portal involvement			0.002
−	62	10	
+	40	24	
Intrahepatic metastasis			<0.001
−	90	17	
+	12	17	

HBV, hepatitis B virus; HCV, hepatitis C virus; NBNC, non-A, non-B fulminant hepatic failure.
[a]*t*-test.

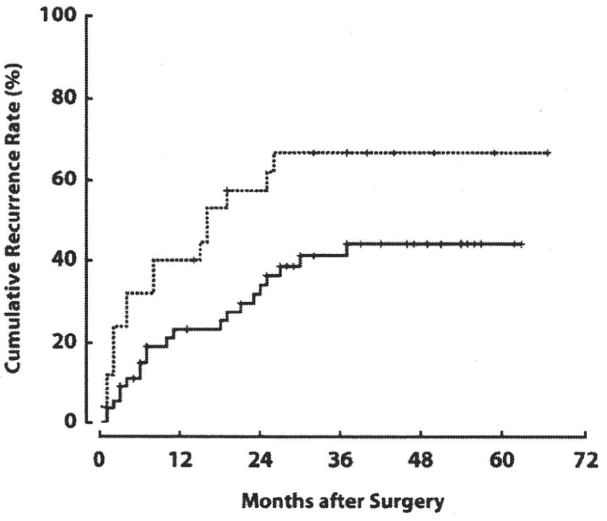

Number at risk

Months	0	12	24	36	48	60
Unchanged	55	37	31	21	14	3
Reduced	25	15	9	6	3	1

Figure 4 Kaplan–Meier curves for time to recurrence. Cumulative recurrence rates (%) of patients with unchanged and reduced TGFBR2 expression are indicated by solid and dotted lines, respectively.

completely abolished in the cell with reduced TGFBR2 expression.

Reduced TGFBR2 expression correlated with portal vain invasion in HCC cases, and poorly differentiated HCC cells showed lower TGFBR2 expression compared with well-differentiated cells. This suggests that HCC cells, with reduced TGFBR2 expression, seem to be more invasive and may promote IM. Recently, Matsuzaki *et al*[38] showed the involvement of the TGF-β receptor-independent, JNK–SMAD3 pathway in HCC progression.[38] The receptor activates SMAD3 by phosphorylation at the C-terminal region, whereas JNK phosphorylates the linker region of SMAD3, which is involved in tumor progression. In HCC cells with reduced TGFBR2 expression, it seems likely that the JNK–SMAD3 pathway may have a dominant role in cancer progression. Further studies are needed to elucidate the function of TGF-β signaling in HCCs with reduced TGFBR2 expression.

Although the role of TGF-β signaling in HCC progression remains controversial, we have shown that the reduced expression of TGFBR2 in HCC correlates significantly with aggressive features, such as IM and short time-to-recurrence. We suggest that reduced TGFBR2 expression may not only be a biomarker for IM, but also a predictive factor for recurrence of HCC.

Supplementary Information accompanies the paper on the Laboratory Investigation website (http://www.laboratoryinvestigation.org)

ACKNOWLEDGEMENTS
This study was supported by Grant-in-aid for Scientific Research on Priority Areas from the Ministry of Education, Culture, Sports, Science, and Technology (MEXT); grants for the Health and Labor Sciences Research and the Third Term Comprehensive 10-Year Strategy for Cancer Control from the Ministry of Health, Labor, and Welfare of Japan; and Research Grants for Life Sciences and Medicine from the Keio University Medical Science Fund.

DISCLOSURE/CONFLICT OF INTEREST
The authors declare no conflict of interest.

1. El-Serag HB. Hepatocellular carcinoma: an epidemiologic view. J Clin Gastroenterol 2002;35:S72–S78.
2. Arakawa M, Kage M, Sugihara S, *et al.* Emergence of malignant lesions within an adenomatous hyperplastic nodule in a cirrhotic liver. Observations in five cases. Gastroenterology 1986;91:198–208.
3. Gressner AM, Weiskirchen R, Breitkopf K, *et al.* Roles of TGF-beta in hepatic fibrosis. Front Biosci 2002;7:d793–d807.
4. Nakamura T, Tomita Y, Hirai R, *et al.* Inhibitory effect of transforming growth factor-beta on DNA synthesis of adult rat hepatocytes in primary culture. Biochem Biophys Res Commun 1985;133:1042–1050.
5. Carr BI, Hayashi I, Branum EL, *et al.* Inhibition of DNA synthesis in rat hepatocytes by platelet-derived type beta transforming growth factor. Cancer Res 1986;46:2330–2334.
6. Massague J, Blain SW, Lo RS. TGFβ signaling in growth control, cancer, and heritable disorders. Cell 2000;103:295–309.
7. Derynck R, Akhurst RJ, Balmain A. TGF-β signaling in tumor suppression and cancer progression. Nat Genet 2001;29:117–129.
8. Siegel PM, Massague J. Cytostatic and apoptotic actions of TGF-β in homeostasis and cancer. Nat Rev Cancer 2003;3:807–821.
9. Markowitz S, Wang J, Myeroff L, *et al.* Inactivation of the type II TGF-beta receptor in colon cancer cells with microsatellite instability. Science 1995;268:1336–1338.
10. Myeroff LL, Parsons R, Kim SJ, *et al.* A transforming growth factor beta receptor type II gene mutation common in colon and gastric but rare in endometrial cancers with microsatellite instability. Cancer Res 1995;55:5545–5547.
11. Park K, Kim SJ, Bang YJ, *et al.* Genetic changes in the transforming growth factor beta (TGF-beta) type II receptor gene in human gastric cancer cells: correlation with sensitivity to growth inhibition by TGF-beta. Proc Natl Acad Sci USA 1994;91:8772–8776.
12. Izumoto S, Arita N, Ohnishi T, *et al.* Microsatellite instability and mutated type II transforming growth factor-beta receptor gene in gliomas. Cancer Lett 1997;112:251–256.
13. Hahn SA, Schutte M, Hoque AT, *et al.* DPC4, a candidate tumor suppressor gene at human chromosome 18q21.1. Science 1996;271:350–353.
14. Kawate S, Takenoshita S, Ohwada S, *et al.* Mutation analysis of transforming growth factor beta type II receptor, Smad2, and Smad4 in hepatocellular carcinoma. Int J Oncol 1999;14:127–131.
15. Yakicier MC, Irmak MB, Romano A, *et al.* Smad2 and Smad4 gene mutations in hepatocellular carcinoma. Oncogene 1999;18:4879–4883.
16. Hirohashi S, Ishak KG, Kojiro M, *et al.* Hepatocellular carcinoma. In: Hamilton SR, Aaltonen LA (eds). Tumours of the Digestive System. IARC Press: Lyon, 2000, pp 159–172.
17. Murakami T. Establishment and characterization of human hepatocellular carcinoma cell line (KIM-1). Acta Hepatol Jpn 1984;25:532–539.
18. Yano H, Maruiwa M, Murakami T, *et al.* A new human pleomorphic hepatocellular carcinoma cell line, KYN-2. Acta Pathol Jpn 1988;38:953–966.
19. Osada T, Sakamoto M, Ino Y, *et al.* E-cadherin is involved in the intrahepatic metastasis of hepatocellular carcinoma. Hepatology 1996;24:1460–1467.
20. Eisen MB, Spellman PT, Brown PO, *et al.* Cluster analysis and display of genome-wide expression patterns. Proc Natl Acad Sci USA 1998;95:14863–14868.
21. Genda T, Sakamoto M, Ichida T, *et al.* Cell motility mediated by rho and rho-associated protein kinase plays a critical role in intrahepatic metastasis of human hepatocellular carcinoma. Hepatology 1999;30:1027–1036.
22. Abou-Shady M, Baer HU, Friess H, *et al.* Transforming growth factor betas and their signaling receptors in human hepatocellular carcinoma. Am J Surg 1999;177:209–215.
23. Kiss A, Wang NJ, Xie JP, *et al.* Analysis of transforming growth factor (TGF)-alpha/epidermal growth factor receptor, hepatocyte growth Factor/c-met, TGF-beta receptor type II, and p53 expression in human hepatocellular carcinomas. Clin Cancer Res 1997;3:1059–1066.
24. Musch A, Rabe C, Paik M, *et al.* Altered expression of TGF-beta receptors in hepatocellular carcinoma—effects of a constitutively active TGF-beta type I receptor mutant. Digestion 2005;71:78–91.
25. Pinto M, Oliveira C, Cirnes L, *et al.* Promoter methylation of TGFbeta receptor I and mutation of TGFbeta receptor II are frequent events in MSI sporadic gastric carcinomas. J Pathol 2003;200:32–38.
26. Zhang HT, Chen XF, Wang MH, *et al.* Defective expression of transforming growth factor beta receptor type II is associated with CpG methylated promoter in primary non-small cell lung cancer. Clin Cancer Res 2004;10:2359–2367.
27. Zhao H, Shiina H, Greene KL, *et al.* CpG methylation at promoter site -140 inactivates TGFbeta2 receptor gene in prostate cancer. Cancer 2005;104:44–52.
28. Nagao T, Inoue S, Goto S, *et al.* Hepatic resection for hepatocellular carcinoma. Clinical features and long-term prognosis. Ann Surg 1987;205:33–40.
29. Nagao T, Inoue S, Yoshimi F, *et al.* Postoperative recurrence of hepatocellular carcinoma. Ann Surg 1990;211:28–33.
30. Yamanaka N, Okamoto E, Fujihara S, *et al.* Do the tumor cells of hepatocellular carcinomas dislodge into the portal venous stream during hepatic resection? Cancer 1992;70:2263–2267.
31. Nakanishi K, Sakamoto M, Yasuda J, *et al.* Critical involvement of the phosphatidylinositol 3-kinase/Akt pathway in anchorage-independent growth and hematogeneous intrahepatic metastasis of liver cancer. Cancer Res 2002;62:2971–2975.
32. Chuma M, Sakamoto M, Yasuda J, *et al.* Overexpression of cortactin is involved in motility and metastasis of hepatocellular carcinoma. J Hepatol 2004;41:629–636.
33. Mazzocca A, Fransvea E, Lavezzari G, *et al.* Inhibition of transforming growth factor beta receptor I kinase blocks hepatocellular carcinoma growth through neo-angiogenesis regulation. Hepatology 2009;50:1140–1151.
34. Mazzocca A, Fransvea E, Dituri F, *et al.* Down-regulation of connective tissue growth factor by inhibition of transforming growth factor beta blocks the tumor-stroma cross-talk and tumor progression in hepatocellular carcinoma. Hepatology 2010;51:523–534.
35. Fransvea E, Angelotti U, Antonaci S, *et al.* Blocking transforming growth factor-beta up-regulates E-cadherin and reduces migration and invasion of hepatocellular carcinoma cells. Hepatology 2008;47:1557–1566.
36. Coulouarn C, Factor VM, Thorgeirsson SS. Transforming growth factor-beta gene expression signature in mouse hepatocytes predicts clinical outcome in human cancer. Hepatology 2008;47:2059–2067.
37. Matsuzaki K, Murata M, Yoshida K, *et al.* Chronic inflammation associated with hepatitis C virus infection perturbs hepatic transforming growth factor beta signaling, promoting cirrhosis and hepatocellular carcinoma. Hepatology 2007;46:48–57.
38. Murata M, Matsuzaki K, Yoshida K, *et al.* Hepatitis B virus X protein shifts human hepatic transforming growth factor (TGF)-beta signaling from tumor suppression to oncogenesis in early chronic hepatitis B. Hepatology 2008;49:1203–1217.

Bmi-1 gene is upregulated in early-stage hepatocellular carcinoma and correlates with ATP-binding cassette transporter B1 expression

Kathryn Effendi,[1,3] Taisuke Mori,[1,3] Mina Komuta,[1] Yohei Masugi,[1] Wenlin Du[1] and Michiie Sakamoto[1,2]

[1]Department of Pathology, School of Medicine, Keio University, Tokyo, Japan

(Received September 29, 2009/Revised October 24, 2009/Accepted November 1, 2009/Online publication January 19, 2010)

Overexpression of "stemness gene" *Bmi-1* has been identified in some solid tumors. We investigated *Bmi-1* expression in hepatocellular carcinoma (HCC) and ATP-binding cassette transporter B1 (*ABCB1*) as a new potential target for *Bmi-1*. *Bmi-1* was highly expressed in HCC cell lines and the most well differentiated cell line, KIM-1, showed the highest expression. Immunohistochemical, immunocytochemical, and immunoelectron microscopic analysis showed the Bmi-1 protein as having a high intensity of small dots within the nucleus which reflected concentrated sites of Bmi-1 repressive activity. Clear "dot-pattern" staining was observed in 24 of 37 (65%) well differentiated HCC (including 13 of 21 early nodules [62%]), in 32 of 71 (45%) moderately differentiated HCC, and 7 of 14 (50%) poorly differentiated HCC. A similar expression was not observed in non-cancerous background regions. High Bmi-1 expression was observed in the early and well differentiated HCC. Furthermore, overexpression and suppression of *Bmi-1* was followed by a respective increase and decrease in *ABCB1* expression. As with *Bmi-1*, high *ABCB1* expression was also observed in the early and well differentiated HCC. A strong correlation between *ABCB1* and *Bmi-1* mRNA expression was seen in HCC cell lines and clinical samples (Pearson's correlation coefficient 0.95 and 0.90, respectively). The *Bmi-1* gene is upregulated in HCC, and in particular is highly expressed in early and well differentiated HCC. The fact that this expression correlated with that of *ABCB1* suggests a new regulation target for *Bmi-1*, and gives new insight into early hepatocarcinogenesis mechanisms and potential targets for future HCC treatment. (*Cancer Sci* 2010; 101: 666–672)

Hepatocellular carcinoma (HCC) is the sixth most common malignancy in the world and still ranks as the third highest cause of cancer-related death globally.[1] Although individual risks for hepatocarcinogenesis, such as hepatitis viral infection, excessive alcohol intake, and non-alcoholic steatohepatitis are well established, a poor prognosis of HCC is still unavoidable due to the unclear mechanism of hepatocarcinogenesis. HCC is characterized by a multistage process of tumor progression,[2] and molecular changes, particularly in the early stage of HCC, have rarely been shown. The idea of using stem cell principles to understand tumor development and progression has emerged because they share similar characteristics. Recent reports on cancer stem cells or acquirement of stem cell-like properties in various tumors have greatly increased the possible connection of these cells in tumorigenesis.[3,4] *Bmi-1* was first identified as a proto-oncogene that cooperates with c-*myc* to generate mouse pre-B cell lymphomas.[5] Some reports show that *Bmi-1* might induce immortalization by regulating human telomerase reverse transcriptase (hTERT) expression,[6–9] and might play a role in tumorigenesis by acting as a negative regulator of the INK4a/ARF locus that encodes two important tumor suppressors in human cancer, *p16* and *p19*.[10,11] The overexpression of *Bmi-1* has been identified in lymphoma[12,13] and in a few solid tumors such as lung, colorectal, nasopharyngeal, bladder, and HCC.[9,14–18] Many reports mainly focus on *Bmi-1* expression in the advanced stages of cancer and its role in a poor prognosis. However, the exact mechanistic role of *Bmi-1* in tumorigenesis is not clear. In HCC, inactivation of *p16* expression, a well-known target of *Bmi-1*, is already observed in the early stages of hepatocarcinogenesis, due to methylation or an epigenetic mechanism.[19,20] This suggests that another target in the *Bmi-1* signaling pathway should exist. Therefore, we examined the involvement of the "stemness gene" *Bmi-1* and its new potential downstream target in hepatocarcinogenesis.

To our knowledge, there are no studies clearly showing a subcellular expression pattern of *Bmi-1* as a high intensity of small dots within the nucleus in cancer cells. Herein, we examined the expression patterns of *Bmi-1* in HCC cell lines and clinical specimens by immunohistochemistry, and these were confirmed with immunocytochemistry and immunoelectron microscopy. We also examined the expression levels of the ATP-binding cassette transporter B1 (*ABCB1*), listed as one of the genes upregulated after *Bmi-1* induction in bone marrow stromal cells.[6] We hypothesize the potential for *ABCB1* to be a new target for *Bmi-1*. Immunohistochemical staining and mRNA expression level of *ABCB1* were analyzed to investigate the correlation between *Bmi-1* and *ABCB1*.

Materials and Methods

Cell culture. The human HCC cell lines, PLC/PRF/5 and HepG2, were obtained from the American Type Culture Collection (Manassas, VA, USA). KIM-1, KYN-2, and Li7 were established as reported previously.[21] All the cells were grown in RPMI-1640 medium supplemented with 10% FBS, 100 U/mL penicillin, and 100 μg/mL streptomycin.

Tissue specimens of HCC. HCCs and corresponding non-cancerous liver tissue were obtained from 100 patients with 122 nodules (37 well differentiated [including 21 early], 71 moderately differentiated, and 14 poorly differentiated HCCs) who underwent surgical resection at Keio University Hospital (Tokyo, Japan) between 2003 and 2006. The specimens were fixed in 10% formalin and embedded in paraffin. Three pathologists evaluated the histological diagnosis according to the criteria set by the World Health Organization.[22] The histological grade for HCC where different types were found within the same nodule was determined by the predominant histological grade. Primary hepatocytes were harvested from the autopsy of a human fetal liver donor with signed, informed consent. The cells were resuspended in growth medium (10% FBS in DMEM, containing 0.1 mM non-essential amino acid and 0.1 mM sodium pyruvate solution; Gibco BRL, Grand Island, NY,

[2]To whom correspondence should be addressed.
E-mail: msakamot@sc.itc.keio.ac.jp
[3]These authors contributed equally to this work.

doi: 10.1111/j.1349-7006.2009.01431.x

USA), and were maintained at 37°C in a humidified atmosphere containing 95% air and 5% CO_2. This study was carried out with the approval of the Ethics Committee of Keio University School of Medicine.

Real-time quantitative RT-PCR. Real-time quantitative RT-PCR (qRT-PCR) analysis was carried out as previously reported,[6] at least three times, including a no-template negative control. A total of 15 (five well differentiated, seven moderately differentiated, and three poorly differentiated) HCC clinical samples were used. The primer sets were: *Bmi-1* forward, 5′-GAGGGTACTTCATTGATGCCACAAC-3′ and reverse, 5′-GCTGGTCTCCAGGTAACGAACAATA-3′; *ABCB1* forward, 5′-GAGGCCAACATACATGCCTTCA-3′ and reverse, 5′-GGC TGTCTAACAAGGGCACGA-3′.

Immunohistochemical and immunocytochemical analysis. Immunohistochemical staining was done on formalin-fixed, paraffin-embedded tissue sections. These were heated at 120°C in 0.01 mol/L sodium citrate buffer, pH 7.0, for 10 min before incubation with a mouse Bmi-1 antibody (1/200; Upstate Biotechnology, Lake Placid, NY, USA) and a multidrug resistance protein 1 (MDR1) antibody (1/200; Santa Cruz Biotechnology, Santa Cruz, CA, USA). Sections were then incubated with ImmPRESS antimouse Ig kit secondary antibody (Vector Laboratories, Burlingame, CA, USA), and stained with diaminobenzidine. For immunocytochemical analysis, KIM-1 cells were grown to confluence on glass slides, fixed, and washed. The slides were incubated with the Bmi-1 antibody (1/200) in PBS containing 1% BSA, followed by FITC-conjugated, antimouse Ig (1/400; Dako, Glostrup, Denmark). Staining was evaluated using the LSM 510 Meta confocal microscope (Carl Zeiss, Oberkochen, Germany). All staining analysis was done at least twice. We defined Bmi-1 staining criteria as follows: distributed diffusely with clear staining of the "dot-pattern" was scored 2+; distributed focally with weak staining of the dot-pattern was scored 1+; and an absence of the dot-pattern was considered negative. Evaluation criteria for ABCB1 were defined as follows: clear staining of irregular canalicular with cytoplasmic staining scored 2+; an irregular canalicular staining pattern scored 1+; and no staining was considered negative.

Immunoelectron microscopy. KIM-1 cells grown to confluence on glass slides were fixed in 4% formaldehyde and incubated overnight at 4°C with the Bmi-1 antibody (1/200). After rinsing they were treated with a mouse secondary antibody (1/100; Dako) for 3 h at room temperature, then re-fixed in 1% glutaraldehyde for 10 min. After further rinsing, the sections were stained with diaminobenzidine and post-fixed in 2% osmium tetroxide. The slides were dehydrated in graded alcohol, embedded in epoxy resin, and hardened at 60°C for 72 h. Ultrathin sections were cut with an ultramicrotome, stained with uranyl acetate and viewed under a JEOL 1200 EXII transmission electron microscope (Nihon Denshi, Tokyo, Japan).

Immunoblotting. PLC/PRF/5, HepG2, KIM-1, KYN-2, and Li7 cells were lysed in lysis buffer (50 mM Tris-HCL [pH 7.5], 150 mM NaCl, 5 mM EDTA, 1% NP-40, and complete protease inhibitors). Supernatants of the homogenates were subjected to NuPAGE (4–12% Bis-Tris gel; Invitrogen, Carlsbad, CA, USA) by electrophoresis, and transferred to PVDF membranes. Anti-Bmi-1 (1/500), anti-MDR1 (1/200), and anti-actin (1/1000; Sigma, St Louis, MO, USA) were hybridized to the membranes and detected with ECL Western blotting detection reagents (GE Healthcare, Amersham, UK).

Transfection-induced overexpression and RNA interference. Human Bmi-1 full coding cDNA was cloned from the KIM-1 cell line with RT-PCR and inserted into pcDNA53 (Invitrogen). This vector was transfected into the primary fetal hepatocytes using Lipofectamine LTX and positive expression vector-transfected cells were selected with G418 (Invitrogen), according to the manufacturer's instructions. For RNA interference, all purified and pre-annealed siRNA molecules were obtained from Takara Bio (Shiga, Japan). Two siRNA molecules were used, siBmi-1#1 and siBmi-1#2, with the targeted sequences 5′-AACAAUAACGAAUAGAAUUGA-3′ and 5′-AA GAAUUAUAACUGAUGAUGA-3′, respectively. Control (non-targeting sequence), unmodified siRNA duplex was also purchased from Takara Bio.

Statistical analysis. Data are expressed as mean ± SEM. The χ^2-test was used when appropriate to determine the correlations between clinicopathological variables and *Bmi-1* expression. The relative mRNA expression levels were compared using the unpaired *t*-test, and the Pearson's correlation coefficient test was also used. Statistical significance was defined as $P < 0.05$. All statistical analyses were carried out using Statcel software version 2.0 (OSM, Tokyo, Japan).

Results

***Bmi-1* expressed in HCC cell lines and distributed in high intensity, dot-pattern expression in nucleus.** To assess the potential role of *Bmi-1* in hepatocarcinogenesis, we examined *Bmi-1* expression in five human HCC cell lines using qRT-PCR and Western blot analysis. *Bmi-1* was highly expressed at both the mRNA and protein level. The most well differentiated HCC cell line, KIM-1, showed at least a three-fold higher level of expression of *Bmi-1*, compared with the other cell lines

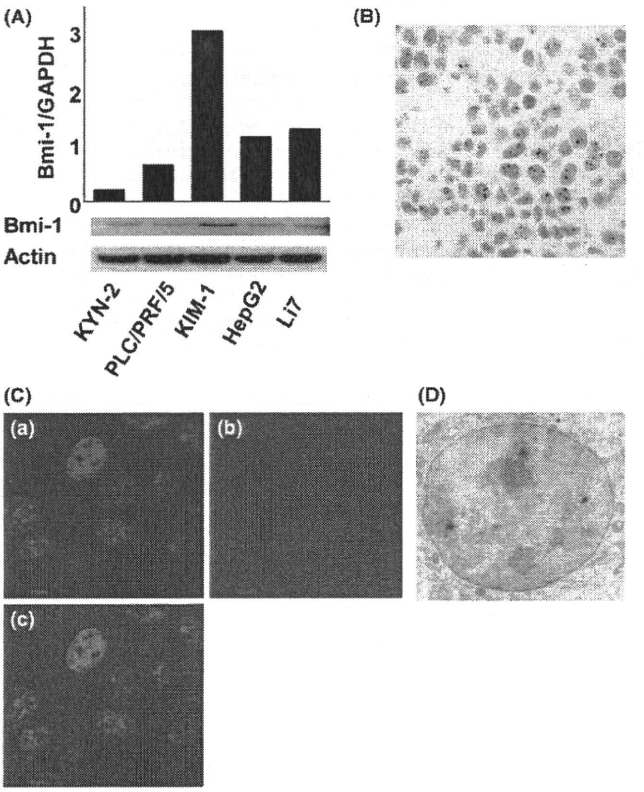

Fig. 1. *Bmi-1* expression in hepatocellular carcinoma (HCC) cell lines. (A) Quantitative real-time- PCR and Western blot of *Bmi-1* in HCC cell lines. *Bmi-1* is significantly expressed in the KIM-1 cell line compared with other cell lines. Nuclear fraction proteins were used in the Western blot analysis. Immunohistochemistry (B) and immuno cytochemistry (C) of KIM-1 cells. Bmi-1 was diffusely distributed intranuclearly (a, DAPI: blue; b, anti-Bmi-1: red; c, merged). (D) Immunoelectron micrograph of KIM-1. Bmi-1 particles are shown as small black dots inside the nucleus.

(Fig. 1A). As a transcriptional repressor, Bmi-1 activity is expected in the nucleus, and we found Bmi-1 protein enrichment in the nuclear fraction compared with the whole lysates (data not shown). Immunohistochemistry, immunocytochemistry, and immunoelectron microscopic of the KIM-1 cells showed that the Bmi-1 protein was distributed in high-intensity aggregates within the nucleus (Fig. 1B–D). These results confirmed localization of the Bmi-1 protein in the nucleus, with a dot-pattern appearance.

***Bmi-1* expressed in HCC clinical samples, particularly in early stage hepatocarcinogenesis.** We evaluated Bmi-1 protein expression in 122 HCC nodules (37 well differentiated [including 21 early nodules], 71 moderately, and 14 poorly differentiated HCCs). As with Bmi-1 expression in the HCC cell lines, Bmi-1 expression in clinical samples was observed as small dots distributed inside the nucleus (Fig. 2A), but the Bmi-1 dot-pattern expression was not observed in the surrounding liver tissue (Fig. 2B). There was no correlation between expression of Bmi-1 and clinicopathological parameters, such as age, gender, portal involvement, intrahepatic metastasis, etiology, or non-cancerous background liver tissue. However, Bmi-1 positive expression was significantly associated with well (including early) differentiated HCC ($P = 0.023$) (Table 1). A 2+ score was observed in 24 of the 37 (65%) well differentiated HCCs (including 13 of the 21 early nodules [62%]), 32 of the 71 (45%) moderately differentiated HCCs, and 7 of the 14 (50%) poorly differentiated HCCs. In contrast, negative expression was observed in only 2 of the 37 (5%) well differentiated HCCs (including 2 of the 21 early nodules [10%]), 15 of the 71 (21%) moderately differentiated HCCs, and 4 of the 14 (29%) poorly differentiated HCCs (Table 2). Interestingly, a higher level of Bmi-1 expression was observed in the early and well differentiated HCCs, and this declined with the progression of HCC. Similar findings were found using qRT-PCR from clinical tissue samples. Strongly positive *Bmi-1* expression was observed in the five well differentiated HCC cases, compared with the seven moderately differentiated cases and the three poorly differentiated HCC cases (Fig. 2C). The average level of *Bmi-1* expression was significantly higher in tumor tissue compared with the non-cancerous background liver tissue (2.23 *vs* 0.86; $P = 0.002$).

***Bmi-1* expression linked to *ABCB1* expression.** We have previously analyzed gene expression profiles after *Bmi-1* induction in bone marrow stromal cells.[6] Among the genes upregulated we found that the *ABCB1* gene was upregulated together with the overexpression of *Bmi-1*, compared with the control parental cells (T. Mori *et al.*, unpublished observation, 2004). To further verify the regulation of *ABCB1* we looked at changes in *ABCB1* expression during transient overexpression of *Bmi-1* using primary fetal hepatocytes. Following *Bmi-1* overexpression, relative mRNA levels of *ABCB1* in primary fetal hepatocytes were increased threefold (Fig. 3A). *Bmi-1* knockdown also led to a downregulation of *ABCB1* expression in the KIM-1 HCC cell line (Fig. 3B), however, decreased *ABCB1* expression was not very significant, which might be due to the presence of *Bmi-1*-independent *ABCB1* expression. These results suggest a parallel association between *Bmi-1* and *ABCB1* expression in HCC cell lines and hepatocytes.

***ABCB1* expression in HCC cell lines and HCC clinical samples correlated with *Bmi-1* expression.** We further evaluated *ABCB1* expression in HCC cell lines and clinical samples. As with *Bmi-1*, the highest levels of ABCB1 mRNA and protein expression were observed in KIM-1 cells, relative to the other cell lines. *ABCB1* mRNA expression level in tumor tissue is not significantly higher compared with non-cancerous background liver tissue due to its normal expression in non-cancerous background liver tissue, however, there is a tendency for higher expression level of *ABCB1* in well differentiated cases (2.30 *vs* 1.53; $P = 0.21$) (Fig. S1a,b). We found a strong statistical correlation between *ABCB1* and *Bmi-1* mRNA expression with the Pearson's correlation coefficient being 0.95 and 0.90 for HCC cell lines and HCC clinical samples, respectively (Fig. 4A,B). Immunohistochemical staining of ABCB1 showed both cytoplasmic and a canalicular staining pattern in the tumor region. Although the canalicular staining pattern was also seen in the surrounding non-cancerous region, the pattern was more irregular and thicker (Fig. S1c,d). A 2+ score was observed in 29 of 37 (78%) well differentiated HCCs (including 18 of 21 early differentiated nodules [86%]), in 50 of 71 (70%) moderately differentiated HCCs, and in 10 of 14 (71%) poorly differentiated HCCs. Negative expression was observed in 1 of 37 (3%) well differentiated HCCs (no early nodules had negative expression),

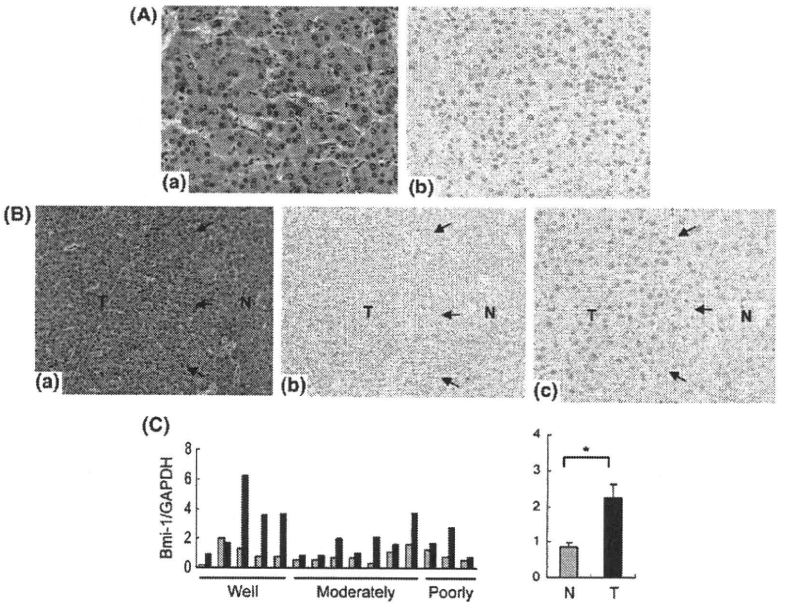

Fig. 2. *Bmi-1* expression in hepatocellular carcinoma (HCC) clinical samples. (A) Immunostaining of Bmi-1 in moderately differentiated HCC. Magnification, ×200. A clear dot-pattern of Bmi-1 was distributed diffusely in the tumor region. (B) Boundary region of well differentiated HCC (a, H&E stain; b, corresponding Bmi-1 staining, magnification ×100; c, magnification ×200). Bmi-1 expression was observed in the tumor region but not in surrounding liver tissue. Black arrows outline the border between the non-cancerous background region (N) and the tumor region (T). (C) *Bmi-1* mRNA expression levels in HCC clinical cases. The relative mRNA expression levels in tumor tissues (black bar, T) and corresponding non-cancerous, background liver tissues (gray bar, N) (left panel). High *Bmi-1* expression was observed in well differentiated HCC. The average expression level of *Bmi-1* was significantly higher in tumor tissues than in non-cancerous, background liver tissues (2.23 *vs* 0.86; *$P = 0.002$) (right panel).

doi: 10.1111/j.1349-7006.2009.01431.x

Table 1. Characteristics of 122 hepatocellular carcinoma nodules on the basis of Bmi-1 immunostaining

Characteristics	Bmi-1 expression		*P* value
	2+/1+	–	
No. of nodules	101	21	0.339
Mean age (years)	62.7	60.2	NA
Gender			
Male	88	15	NA
Female	13	6	
Tumor size (cm)			
<2	37	6	0.482
≥2	64	15	
Differentiation			
Well (early)	35 (19)	2 (2)	0.023*
Moderately/poorly	66	19	
Portal involvement			
–	54	9	0.376
+	47	12	
Intrahepatic metastasis			
–	80	14	0.214
+	21	7	
Etiology			
Hepatitis B virus	21	7	NA
Hepatitis C virus	61	12	
Non-B / Non-C	19	2	
Non-cancerous liver			
Liver cirrhosis	51	10	0.810
Others	50	11	

*$P < 0.05$. –, absence of dot-pattern staining; 1+, distributed focally with weak dot-pattern staining; 2+, distributed diffusely with clear dot-pattern staining; NA, not available.

Table 2. Immunohistochemical analysis of Bmi-1 expression in hepatocellular carcinoma (HCC) (n = 122)

Histology	Bmi-1 staining score		
	2+	1+	–
Well differentiated HCC (n = 37)	24 (65%)	11 (30%)	2 (5%)
Early HCC (n = 21)	13 (62%)	6 (29%)	2 (10%)
Moderately differentiated HCC (n = 71)	32 (45%)	24 (34%)	15 (21%)
Poorly differentiated HCC (n = 14)	7 (50%)	3 (21%)	4 (29%)

–, absence of dot-pattern staining; 1+, distributed focally with weak dot-pattern staining; 2+, distributed diffusely with clear dot-pattern staining.

in 5 of 71 (7%) moderately differentiated HCCs, and in 3 of 14 (21%) poorly differentiated HCCs (Table 3). As expected, ABCB1 expression was also higher in the well differentiated HCCs. There was a correlation in ABCB1 and Bmi-1 staining (Fig. 4C), and 50 of 122 (41%) cases showed strong expression of both Bmi-1 and ABCB1 (Table 4).

Discussion

Following the identification of *Bmi-1* overexpression in solid tumors,[9,14–16] some studies have also reported the overexpression of *Bmi-1* in HCC.[17,18,23] However, the *Bmi-1* localization area and whether *Bmi-1* is highly expressed in the early or late progression of HCC is still controversial. In this study, high levels of *Bmi-1* expression were observed in early HCC, and we carefully describe the specific subcellular expression of *Bmi-1* within the nucleus. We believe that as a transcriptional repressor, *Bmi-1* activity is expected to occur inside the nucleus.[10,24,25] Moreover, we found a correlation in the expression of *Bmi-1* and *ABCB1* suggesting that *ABCB1* might present a novel downstream target for *Bmi-1*.

Bmi-1 belongs to the Polycomb gene group (PcG) involved in maintaining target genes in their transcriptional state. A possible mechanism of PcG-mediated repression is the recruitment of certain regulatory factors, or chromatin-modifying activities, into a unique nuclear domain which results in inhibiting chromatin remodeling required for the transcriptional process.[24] Indeed, there is evidence showing that 3D imaging of PcG proteins in Drosophila embryos shows distribution of PcG complexes throughout the nuclear volume as discrete loci, which might reflect sites of repressive complexes.[25] In accordance with previous reports, we observed that *Bmi-1* was expressed as high-intensity, small aggregates distributed inside the nucleus in the HCC region. The *Bmi-1* dots appeared in different parts of the nucleus, often very near to or partially coincident with heterochromatin. These findings support the indication of *Bmi-1* function as a gene transcriptional repressor by regulating chromatin silencing. Regarding this immunohistochemical staining dot-pattern as a positive expression of *Bmi-1*, we found high levels of *Bmi-1* expression in well (included early) differentiated HCCs, whereas similar expression was not observed in the corresponding non-cancerous background hepatocytes.

The *Bmi-1* signaling pathway is one of the candidates that might, in part, govern stem cell fate, and acquirement of its "stemness" function has been linked to neoplastic proliferation.[4,26] The ability of *Bmi-1* to promote tumorigenesis and bypass senescence through regulation of *p16* and hTERT expression[6–9] suggests a potential role of *Bmi-1* in initiating hepatocarcinogenesis and immortalization of the hepatocyte.

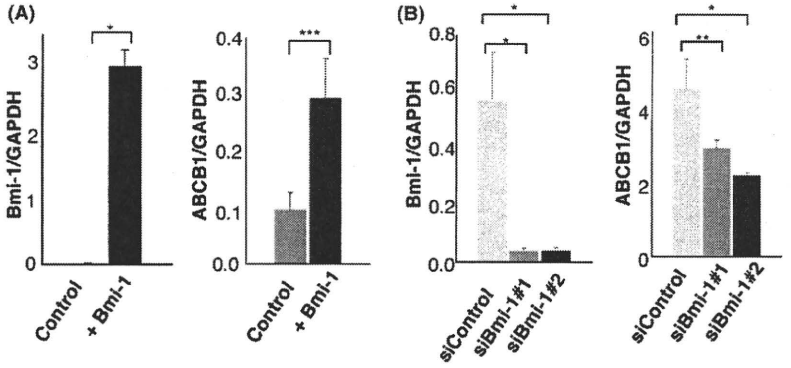

Fig. 3. Overexpression and silencing of *Bmi-1* expression affected ATP-binding cassette transporter B1 (*ABCB1*) expression in primary fetal hepatocytes and a hepatocellular carcinoma (HCC) cell line. (A) *Bmi-1* overexpression in primary fetal hepatocytes resulted in increased *ABCB1* expression, compared with the mock-transduced control (*$P < 0.01$; ***$P = 0.038$). (B) Silencing of *Bmi-1* expression by two different siRNAs (#1 and #2) in KIM-1 cells was followed by a decrease in *ABCB1* expression (*$P < 0.01$; **$P = 0.08$). Error bars were derived from three independent experiments.

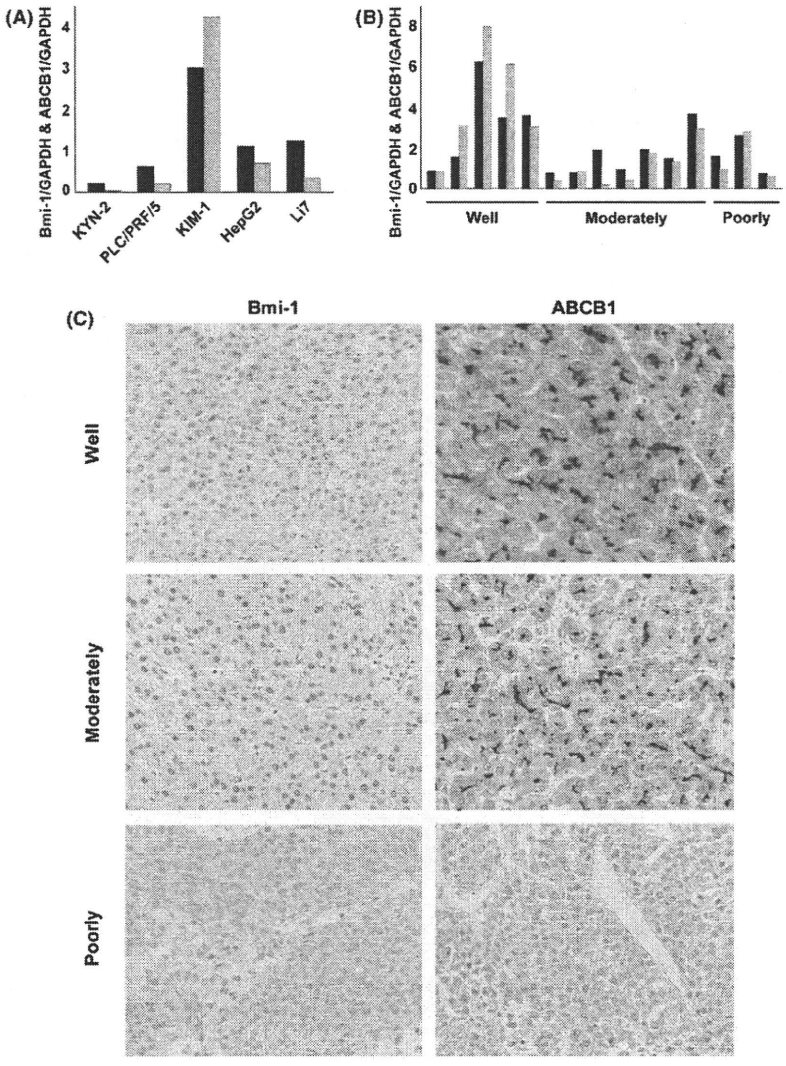

Fig. 4. Correlation and immunostaining of *Bmi-1* and ATP-binding cassette transporter B1 (*ABCB1*) expression in hepatocellular carcinoma (HCC). (A and B) Evaluation of *Bmi-1* and *ABCB1* mRNA expression in HCC cell lines and HCC clinical samples. A strong correlation between *Bmi-1* and *ABCB1* expression was observed in HCC cell lines and clinical samples by the Pearson's correlation coefficient test (0.95, $P = 0.01$; and 0.90, $P < 0.01$, respectively) (black column, *Bmi-1*; gray column, *ABCB1*). (c) Bmi-1 and ABCB1 expression in early, moderately, and poorly differentiated HCC (magnification, ×200). Clear staining of Bmi-1 "dot-pattern" (scored as 2+), and a canalicular and cytoplasmic ABCB1 staining pattern (scored as 2+), was observed in well differentiated HCC. Bmi-1 expression appeared weaker (scored as 1+), and only a canalicular staining pattern of ABCB1 (scored as 1+), was seen in moderately differentiated HCC. No dot-pattern of Bmi-1 and an absence of ABCB1 staining were observed in poorly differentiated HCC (scored as negative). Both Bmi-1 and ABCB1 expression decreased with the progression of HCC, suggesting their correlated expression.

Table 3. Immunohistochemical analysis of ATP-binding cassette transporter B1 (ABCB1) expression in hepatocellular carcinoma (HCC) (n = 122)

Histology	ABCB1 staining score		
	2+	1+	–
Well differentiated HCC (n = 37)	29 (78%)	7 (19%)	1 (3%)
Early HCC (n = 21)	18 (86%)	3 (14%)	0 (0%)
Moderately differentiated HCC (n = 71)	50 (70%)	16 (23%)	5 (7%)
Poorly differentiated HCC (n = 14)	10 (71%)	1 (7%)	3 (21%)

–, no staining; 1+, irregular canalicular staining pattern; 2+, clear staining of irregular canalicular with cytoplasmic staining.

Table 4. Combined immunohistochemical analysis of *Bmi-1* and ATP-binding cassette transporter B1 (ABCB1) expression in hepatocellular carcinoma

ABCB1 staining score Bmi-1 staining score	2+	1+	–
2+	50 (41%)	12 (10%)	1 (1%)
1+	28 (23%)	7 (6%)	3 (2%)
–	11 (9%)	5 (4%)	5 (4%)

ABCB1 staining scores: –, no staining; 1+, irregular canalicular staining pattern; 2+, clear staining of irregular canalicular with cytoplasmic staining. Bmi-1 staining scores: –, absence of dot-pattern staining; 1+, distributed focally with weak dot-pattern staining; 2+, distributed diffusely with clear dot-pattern staining.

Low levels of *p16* expression and increased activation of hTERT have also been reported in HCC, including in early HCC.[19,27,28] We observed high levels of *Bmi-1* expression in early HCC, which might indicate an indispensable function for *Bmi-1* in the early development of cancer. *Bmi-1* expression was also observed in progressed HCC, however, the expression level was not as high as in early HCC. This findings suggested *de novo* tumor development pathways as well as indicated another functional role of *Bmi-1* in progressed HCC. Although it is clear that *Bmi-1* plays a role in keeping self-renewal ability and proliferation, the exact molecular mechanism of *Bmi-1* in early hepatocarcinogenesis remains unclear. Inactivation of *p16* expression by methylation or epigenetic mechanisms has already been observed as an early

doi: 10.1111/j.1349-7006.2009.01431.x